EFFECT OF DUTY CYCLE ON THE PROPERTIES OF VANADIUM OXIDE THIN FILMS DEPOSITED BY PULSED DC REACTIVE MAGNETRON SPUTTERING

Master of Science Thesis

Sinan ÖZGÜN

Eskişehir, 2018

EFFECT OF DUTY CYCLE ON THE PROPERTIES OF VANADIUM OXIDE THIN FILMS DEPOSITED BY PULSED DC REACTIVE MAGNETRON SPUTTERING

Sinan ÖZGÜN

MASTER OF SCIENCE THESIS

Material Science and Engineering Department

Supervisor: Prof. Dr. Ramis Mustafa ÖKSÜZOĞLU

Eskişehir

Anadolu University

Graduate School of Sciences

February, 2018

This thesis study was supported by Technological Research Council of Turkey (TUBITAK) within the scope of 1001 project with Project No: 213M494

FINAL APPROVAL FOR THESIS

This thesis titled “Effect of Duty Cycle on the Properties of Vanadium Oxide Thin Films Deposited by Pulsed DC Reactive Magnetron Sputtering” has been prepared and submitted by Sinan Özgün in partial fulfillment of the requirements in “Anadolu University Directive on Graduate Education and Examination” for the Degree of Master of Science in Material Science and Engineering has been examined and approved on 08/02/2018.

Committee Members		**Signature**
Member (Supervisor)	: Prof. Dr. Ramis Mustafa ÖKSÜZOĞLU	.....
Member	: Prof. Dr. Hasan Hüseyin ERKAYA	.....
Member	: Doç. Dr. Erhan AYAS	.....

.....

Director

Graduate School of Science

ÖZET

GÖREV DÖNGÜSÜ ÜRETİM PARAMETRESİNİN ATMALI DC REAKTİF MAGNETRON SIÇRATMA TEKNİĞİ İLE ÜRETİLMİŞ VANADYUM OKSİT İNCE FİLMLERİN ÖZELLİKLERİNE ETKİSİ

Sinan ÖZGÜN

Malzeme Bilimi ve Mühendisliği Anabilim Dalı

Anadolu Üniversitesi, Fen Bilimleri Enstitüsü, Şubat 2018

Danışman: Prof. Dr. Ramis Mustafa ÖKSÜZOĞLU

Vanadyum oksit dört temel oksit formuna sahip amfoterik bir malzemedir. Vanadyum oksit ince filmlerin özellikleri bu dört temel fazın ve ara fazların yapı içerisindeki miktar ve dağılımlarına bağlı olarak değişmektedir ve bu sayede farklı uygulama alanlarında kullanılabilmektedir. Fiziksel buhar biriktirme yöntemlerinden biri olan atmalı DC reaktif magnetron sıçratma tekniği ile farklı fazlar ve bu fazların birbirlerine oranlarının ayarlanmasında etkili parametrelerden biri de güç kaynağı görev döngüsüdür. Bu tez çalışması güç kaynağı görev döngüsünün vanadyum oksit ince filmlerin özelliklerine etkisinin incelenmesi amacıyla yapılmıştır. Çalışmada %10 ile %32,5 görev döngüsü değerleri arasında üretilen ince filmler üzerinde elektriksel özellikler, yüzey özellikleri ve kristalografik özellikler ile görev döngüsü parametresi arasındaki ilişki incelenmiştir. Elektriksel karakterizasyon sonuçları görev döngüsü ile elektriksel direnç ve özdirenç arasında ters ilişki olduğunu göstermiştir. Elde edilen sonuçlar seçilen alana uygun vanadyum oksit ince filmin büyütülmesi için gereken özelliklere uygun olan görev çevrimi parametresinin belirlenmesine katkı sağlamaktadır.

Anahtar Sözcükler: Görev döngüsü, Vanadyum oksit, Atmalı DC reaktif magnetron sıçratma.

ABSTRACT

EFFECT OF DUTY CYCLE ON THE PROPERTIES OF VANADIUM OXIDE THIN FILMS DEPOSITED BY PULSED DC REACTIVE MAGNETRON SPUTTERING

Sinan ÖZGÜN

Department of Materials Science and Engineering
Anadolu University, Graduate School of Science, February 2018

Supervisor: Prof. Dr. Ramis Mustafa ÖKSÜZOĞLU

Vanadium oxide is an amphoteric material with four principal oxide forms. Properties of vanadium oxide thin films depend on the amount and distribution of these four principal oxides and intermediate phases thus providing different application areas. One of the effective parameters that can adjust the composition and distribution of the phases in pulsed DC reactive magnetron sputtering is the duty cycle of the power source. The aim of this thesis study is to investigate the effect of duty cycle on the properties of vanadium oxide thin films deposited by pulsed DC reactive magnetron sputtering. Electrical properties, surface properties and crystallographic properties of films deposited using duty cycles between 10% and 32,5% are measured to determine the relationship between the properties and the duty cycle. Electrical characterization results indicate that resistance and resistivity of the vanadium oxide thin films are inversely proportional with duty cycle. The results contribute to the appropriate duty cycle determination for deposition of vanadium oxide thin films for chosen application.

Keywords: Duty cycle, Vanadium oxide, Pulsed DC reactive magnetron sputtering.

PREFACE

Working on this master's thesis provided me an invaluable experience. It would not have been possible to finish this work without the support and guidance of brilliant minds around me. I would like to thank some of those amazing people here.

Foremost, I would like to express my thanks to my supervisor Prof. Dr. Ramis Mustafa Öksüzoğlu for his patience, and continuous support of my study and research activities with his immense knowledge. I could never have finished my research without his guidance.

As well as my advisor, I would like to thank my colleagues in Anadolu University Advanced Technology Thin Film Laboratory, Ahmet Murat Yağci, Emrah Dirican, Ercan Şener, Rifat Kaçar, Can Yavru, Erdal Volkan Batur and Gökçe Nur Çakmak.

Furthermore, I would like to express my gratitude to Anadolu University Materials Science & Engineering Department and Graduate School of Science for the financial, academic and technical support.

Last and remarkable, I would like to thank my family for their limitless support, encouragement and patience.

Sinan ÖZGÜN

08/02/2018

STATEMENT OF COMPLIANCE WITH ETHICAL PRINCIPLES AND RULES

I hereby truthfully declare that this thesis is an original work prepared by me; that I have behaved in accordance with the scientific ethical principles and rules throughout the stages of preparation, data collection, analysis and presentation of my work; that I have cited the sources of all the data and information that could be obtained within the scope of this study, and included these sources in the references section; and that this study has been scanned for plagiarism with "scientific plagiarism detection program" used by Anadolu University, and that "it does not have any plagiarism" whatsoever. I also declare that, if a case contrary to my declaration is detected in my work at any time, I hereby express my consent to all the ethical and legal consequences that are involved.

.....

Sinan ÖZGÜN

TABLE OF CONTENTS

Page

LIST OF TABLES

Page

LIST OF FIGURES

Page

SYMBOLS AND ABBREVIATIONS

θ	: Theta
Ω	: Ohm
ω	: Omega
ρ_s	: Sheet resistance
AC	: Alternating Current
AFM	: Atomic Force Microscope
BF	: Bright field
C	: Correction factor
D	: Duty cycle
DC	: Direct Current
DF	: Dark field
FPP	: Four Point Probe
GI-XRD	: Grazing Incidence X-Ray Diffraction
I	: Current
IUPAC	: International Union of Pure and Applied Chemistry
MIT	: Metallic to Insulator Transition
MS	: Magnetron Sputtering
O_2/Ar ratio	: Oxygen gas to Argon gas ratio
P	: Power
P-DC	: Pulsed-Direct Current
P-DC RMS	: Pulsed-Direct Current Reactive Magnetron Sputtering
PDT	: Pulse duration time, pulse on time
PVD	: Physical Vapor Deposition
Ra	: Mean surface roughness

RAFS : Rubidium Frequency Standard

R_c : Contact resistance

R_i : Resistance at room temperature

RF : Radio Frequency

RMS : Root Mean Square

R_p : Electrical Resistance of FPP pins

R_s : Surface resistance

R_{sp} : Spreading resistance

T : Period

t : Time

sccm : Standard Cubic Centimeters per Minute

Si/Si_3N_4 : Silicon nitride coated silicon

Si/SiO_2 : Silicon dioxide coated silicon

STM : Scanning Tunneling Microscope

TCR : Temperature Coefficient of Resistance

TEM : Transmission Electron Microscope

T_i : Initial temperature

T_s : Last temperature

TV : Television

UHV : Ultra High Vacuum

UNAM : National Nanotechnology Research Center

V : Voltage

XRD : X-Ray Diffraction

1. INTRODUCTION AND LITERATURE REVIEW

The aim of this study is to determine the effect of duty cycle on the properties of vanadium oxide thin films deposited by pulsed DC reactive magnetron sputtering (P-DC RMS) onto silicon nitride coated silicon (Si/Si_3N_4) substrates. Also effect of oxygen gas to argon gas ratio (O_2/Ar) on average grain size and surface roughness is inspected along with differences between silicon dioxide coated silicon (Si/SiO_2) and Si/Si_3N_4 substrates for O_2/Ar ratio and substrate selection studies.

Sputtering is one of the many physical vapor deposition (PVD) techniques. It is a widely preferred method for compound thin film deposition as it provides uniform coverage on substrates and a considerably well adhesion with strict control over stoichiometry in materials such as oxides and alloys. It uses energetic particle bombardment of the target to eject material with a plasma formed in vacuum that also acts as a containment and transportation media. Ejected material travels along the plasma and finally deposits on the substrate and its surroundings. To increase the deposition rate and efficiency, magnetic and electric fields are added to the system creating magnetron sputtering. Magnetic or electrical fields employed in the system provides directional control over the plasma and charged particles.

Sputtering is also a flexible technique; different types of sputtering processes are developed for a variety of materials and process routes. DC sputtering is appropriate for metals, RF sputtering enables utilization of insulator targets such as oxides. Magnetron sputtering (MS), which can be used with either a DC or an RF power source helps localizing electron path near to the target. This provides a higher sputtering rate and uniform bombardment of the target surface. Reactive sputtering, on the other hand, makes depositing oxides, nitrides, sulfides and carbides from a metallic target and reactive gas possible. Plasma needed for the sputtering process is created by an inert gas such as argon, and when a reactive gas such as oxygen is introduced into the plasma, reaction occurs between the ejected target material and the reactive gas resulting in a compound deposition onto the substrate. This process is called as reactive sputtering. By controlling the power, pressure and the reactive gas flow it is possible to isolate certain compounds or depositing a mixture of compounds.

In this study the material under investigation is vanadium oxide, an amphoteric material with four primary oxide types and many metastable, intermediate phases. Each

of these oxides feature different properties. Mixing these in certain proportions and structural arrangements gives rise to many applications.

One of the appropriate techniques for depositing vanadium oxide thin films from a high purity vanadium target is DC reactive MS. The problem with the DC power source is the charge build up on the target material resulting in arcs that creates defects on the film. Using a pulsed DC power source prevents charging and arc formation. Duty cycle adjustment allows modification of pulse characteristics, thus may have an effect on the properties of the deposited material.

Other studies show that arcing in reactive MS of dielectrics can be prevented by controlling duty cycle, and pulsing parameters affect substrate conditions and deposition rate by enabling the user to decrease oxidation of target surface [1][2]. Another study on AlCrN thin films states that duty cycle has a considerably high effect on the microstructure and has the ability to alter it from coarse to fine columnar structure [3]. Study on a-C/a-C:Ti multilayer films shows tribological properties significantly depend on the duty cycle [4]. Another study on ZrN thin films proves that duty cycle can alter stoichiometry and effects mechanical properties [5].

Studies on vanadium oxide thin films demonstrate that duty cycle of the power source affects surface morphology, composition and electrical properties of the vanadium oxide thin films by altering the amount of sputtered material into the plasma thus changing reactivity [6].

1.1. Pulsed DC Reactive Magnetron Sputtering

Main working principal of PVD is detaching material into gaseous form from a solid or liquid source named as the target and then condensing the vapor on a surface named as the substrate. Selection of the power supply is an important issue for the sputtering. DC and RF sources are commonly used, but for reactive processes pulsed-DC proved to be a novel power supply technique that prevents arcing and target poisoning. This is accomplished by applying a reverse voltage resulting in discharge of charge build up on the target material.

By combining the advantages of magnetron apparatus and pulsed DC power modulation a highly efficient sputtering process for insulating or semiconductor thin film deposition became possible, the pulsed-DC reactive magnetron sputtering (P-DC RMS).

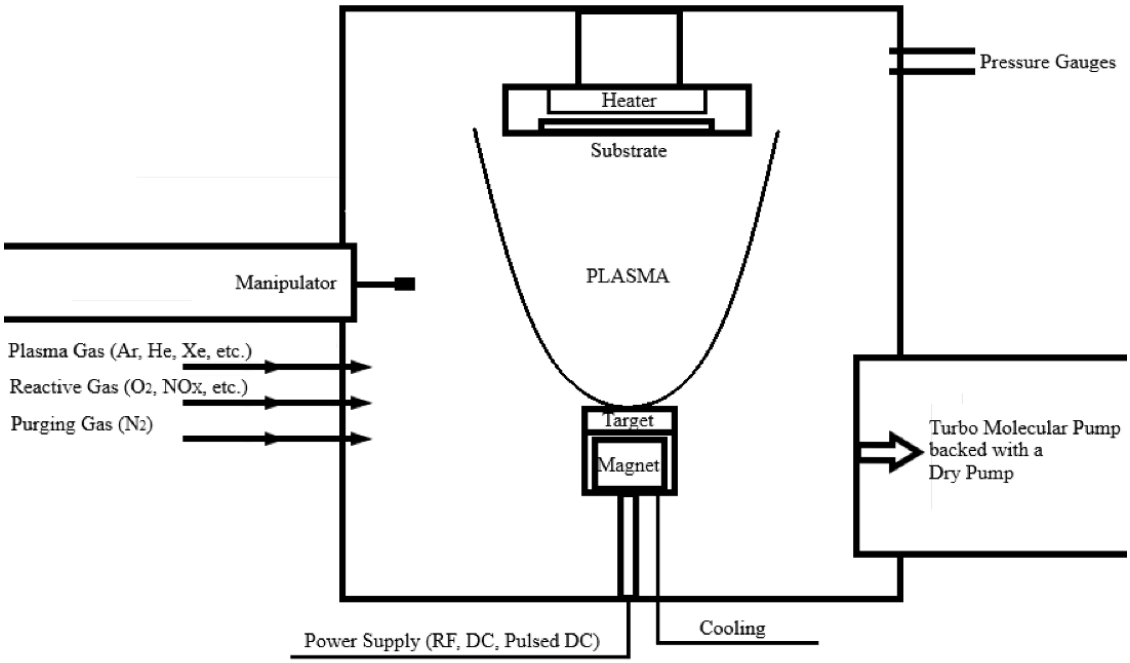

Figure 1.1. *General set-up for a reactive magnetron sputtering system*

In this study an ultra-high vacuum (UHV) MS System with pulsed DC power supply, designed by Prof. Dr. Ramis Mustafa Öksüzoğlu, located in Anadolu University Advanced Technology Thin Film Laboratory is used.

Figure 1.2. *UHV Sputtering System (Anadolu University Advanced Technology Thin Film Laboratory)*

1.1.1. Duty Cycle in Pulsed DC Power Supplies

An important parameter for P-DC RMS technique is the duty cycle which defines the power, current or voltage duration (depending on the modulation type) within a period of the cycle. This affects the charge build up on the target and as a result it may influence the properties of the deposited film. Pulsed DC power supplies provide a means for reactive MS processes to have a higher deposition rate and reduced risk of arc formation.

The difference between a conventional DC power supply and a pulsed DC supply is the frequency. Theoretically speaking a pure DC current has no frequency, but a current converted from AC to DC shows pulsating behavior and when this pulsation is induced deliberately it is called as pulsed-DC. Pulsed DC supplies work in pulse-on and pulse-off cycles. And the ratio of pulse-on time (PDT) divided by the total period (T) gives the duty cycle (D, expressed in %).

$$D = \frac{PDT}{T} x100\% \tag{1.1}$$

Pulsed DC and pulsating DC terms are often used interchangeably but in fact pulsed and pulsating are different phenomena. The difference between signal types are illustrated at Figure 1.3.

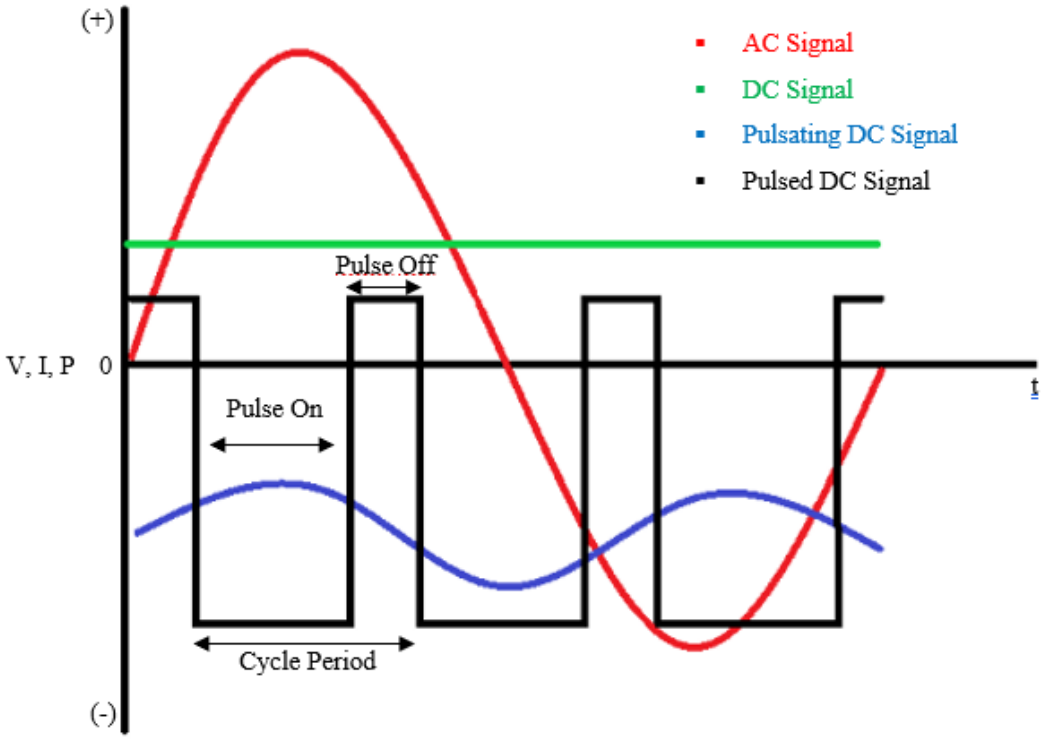

Figure 1.3. *Signal types*

1.2. Vanadium Oxide Thin Films

In most technological applications as well as in thin films, oxides of vanadium are used. Vanadium oxide is an amphoteric oxide with common oxidation states 5, 4, 3, 2, 0. The four principal oxides are V_2O_5, VO_2, V_2O_3, and VO [7][8]. It has more than 20 varieties, including VO, V_2O_3, VO_2, V_3O_5, V_6O_{11}, V_4O_9, and V_2O_5 [9]. The sputter deposited mixed phase vanadium oxide thin films are a combination of these wide variety of oxides. The properties required for applications can be obtained by adjusting the fractions of these phases in thin films.

Many principal oxides of vanadium, especially VO_2 and V_2O_5, have many interesting characteristics due to the partially filled d-orbitals resulting in a wide variety of electronic, optical and catalytic properties that can be applied to a wide range of applications.

Also, the ability of vanadium atoms to possess multiple stable oxidation states results in the easy conversion between oxides of different stoichiometry by oxidation or reduction and is believed to be an important factor for the oxide to function as catalyst in selective oxidation [10].

V_2O_5 called as vanadia or divanadium pentoxide (IUPAC) is the most stable and highly observed oxide form of vanadium. It is an amphoteric oxide with orthorhombic crystal structure where three types of oxygen atoms are present in the lattice: vanadyl oxygen atoms coordinated only to one vanadium atom, bridging oxygen atoms, and the third type is coordinated to two and three vanadium atoms [10].

Another important structural property to be emphasized is the defect structure. It is generally considered that oxygen vacancy is the basic point defect in the V_2O_5 lattice and it is assumed that the vacancy is a double donor which springs from the third oxygen type mentioned before [10].

Also sputter deposited V_2O_5 thin films are a candidate for electrochemical storage devices. The effects of thin film microstructure on capacity-rate performance in V_2O_5 films deposited by RF-MS shows that oriented V_2O_5 films enhance the electrochemical kinetics and films possessing a coarse-grained microstructure exhibited superior rate capability when compared with fine-grained films [11].

Another stable vanadium oxide VO_2 also called vanadium dioxide is an amphoteric oxide with two distinct crystal structures at low and high temperatures. It undergoes a metal-to-semiconductor first-order phase transition at 68°C from the high temperature

tetragonal phase to a low temperature monoclinic form [12]. Due to the amplitude of property changes (resistivity, optical transmission, and reflection in the infrared) during this phase transition VO_2 has many potential applications in electronics and opto-electronics. One fast optical switches based on VO_2 thin films with Au microheaters having switching time about 3 ms have been fabricated [13].

Thin film VO_2 is often of polycrystalline structure with the grain size in the range of 30–120 nm depending strongly on the film growth conditions, single crystal thin film VO_2 can be epitaxially grown on sapphire substrates. The magnitude of the electrical resistance changes during the metallic to insulator transition (MIT) in thin films and the temperature width of the transition are generally not as sharp as it is found in single crystal VO_2 but decreasing the film thickness improves the MIT parameters [14].

In considerable number of applications mixed vanadium oxide (VO_x) thin films are used. One example is the study in RAFS (Rubidium Frequency Standard) which is used in TV broadcasting, telecommunications, and precision measurement systems. Miniaturization of these systems through using VO_x thin films is a promising study area. In one study on VO_x thin film deposited by RF-MS it is shown that the amorphous films consisting of mainly the V_2O_5 and V_2O_3 have flat and stable optical transmittance curves and different thicknesses can be used to adjust the relative optical intensity [15].

1.3. Characterization Techniques

In order to observe the effect of duty cycle on the properties of deposited films three characterization techniques are employed. Grazing Incidence X-Ray Diffraction (GI-XRD) for structural analysis, four-point probe (FPP) for electrical characterization, and atomic force microscopy (AFM) for grain size and surface roughness analysis.

1.3.1. Grazing Incidence X-Ray Diffraction

X-ray diffraction (XRD) technique is used for phase analysis. Working principle is sending X-rays in certain angles onto the sample and to detect the diffracted rays. The obtained Bragg diffraction angles provide information about the crystal structure of the sample. Each material has unique diffraction patterns, by comparing the obtained diffraction pattern with the databases it is possible to define both the material type and the crystal growth direction. In conventional XRD the X-rays are sent to the sample in high angles (θ), in thin films this results in interference between the signals coming from

the sample and the substrate. To overcome the interference GI-XRD has been developed. In this technique X-ray source is kept at a low angle ($0{,}3° < \theta < 1°$), almost parallel to the sample surface, to prevent the X-rays from reaching into the substrate. Instead only the detector revolves on the surface at given 2θ angles, scanning for the diffracted X-rays [16].

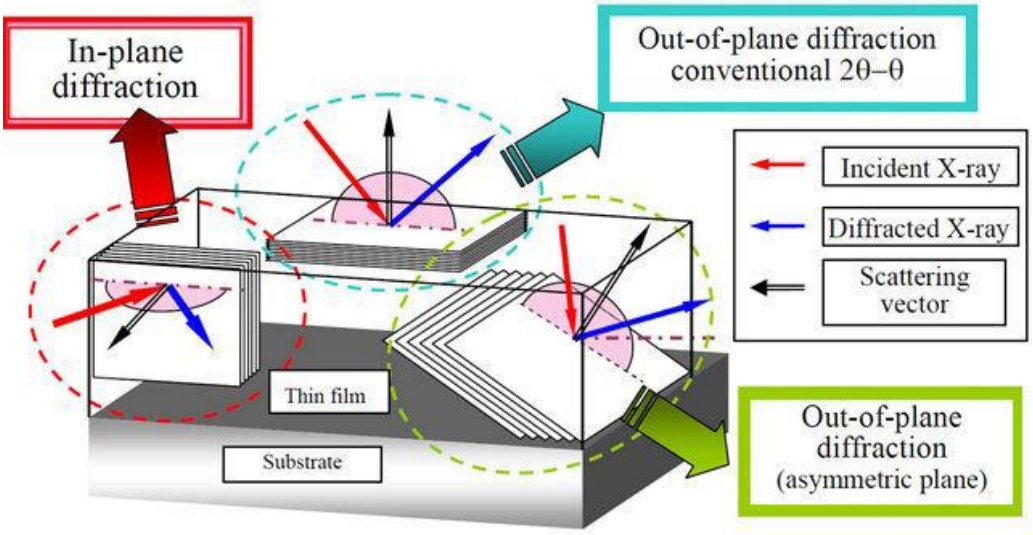

Figure 1.4. *Orientation of crystallographic planes in a thin film sample [17]*

In this study Bruker D8 Advance XRD system with GI-XRD feature is used.

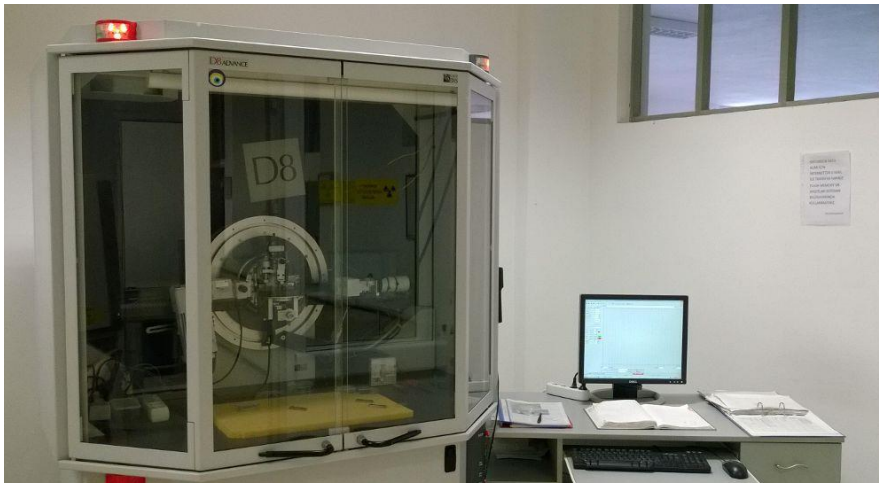

Figure 1.5. *Bruker D8 Advance XRD system (Anadolu University Materials Science and Engineering Department)*

1.3.2. Four Point Probe

FPP technique is used for measuring electrical properties of two dimensional samples such as thin films. It consists of linearly arranged pins with an identical electrical

resistance (R_p). Probes at the ends of line carry the current, two probes at the middle measure the voltage. At the touching point between the probes and the sample contact resistance (R_c) and during the penetration of the current inside the sample spreading resistance (R_{sp}) forms. The sheet resistance (ρ_s) is then calculated with a correction factor consisting of the R_p, R_c, R_{sp} and geometrical factors [18].

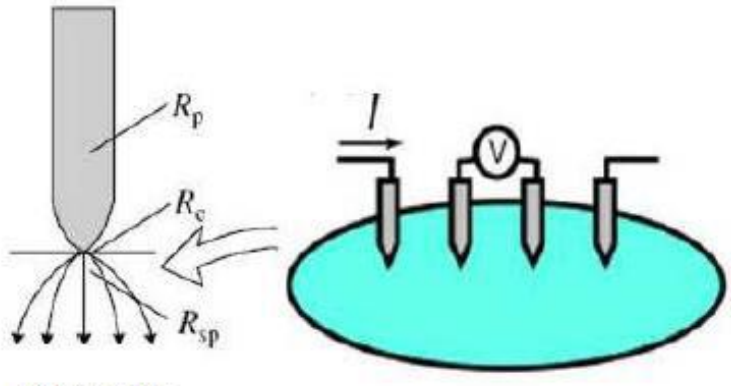

Figure 1.6. *Schematic illustration of FPP technique [18]*

The formula for calculating sheet resistance (ρ_s) is given in Equation 1.2. "C" stands for the correction factor, "V" is the voltage, "I" is the current.

$$\rho_s = \frac{V}{I} C \tag{1.2}$$

Predetermined correction factors (C) for standard shaped samples are listed in Table 1.1. And geometrical factors mentioned in Table 1.1. are explained by illustration in Figure 1.7.

Table 1.1. *Correction factors for ρ_s measurements with FPP [18]*

d/s	circle diam d/s	$a/d = 1$	$a/d = 2$	$a/d = 3$	$a/d \geqq 4$
1.0				0.9988	0.9994
1.25				1.2467	1.2248
1.5			1.4788	1.4893	1.4893
1.75			1.7196	1.7238	1.7238
2.0			1.9454	1.9475	1.9475
2.5			2.3532	2.3541	2.3541
3.0	2.2662	2.4575	2.7000	2.7005	2.7005
4.0	2.9289	3.1137	3.2246	3.2248	3.2248
5.0	3.3625	3.5098	3.5749	3.5750	3.5750
7.5	3.9273	4.0095	4.0361	4.0362	4.0362
10.0	4.1716	4.2209	4.2357	4.2357	4.2357
15.0	4.3646	4.3882	4.3947	4.3947	4.3947
20.0	4.4364	4.4516	4.4553	4.4553	4.4553
40.0	4.5076	4.5120	4.5129	4.5129	4.5129
∞	4.5324	4.5324	4.5324	4.5325	4.5324

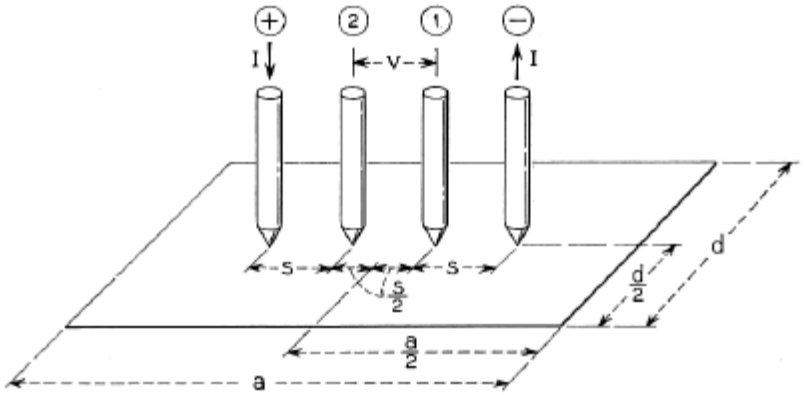

Figure 1.7. *Geometric factors for FPP measurements [18]*

Another important electrical property, temperature coefficient of resistance (TCR) can also be measured with FPP technique by integrating a heater with temperature controller and a thermocouple to see the temperature of the sample. For measurements at short temperature increments TCR can be calculated with Equation 1.3 [18].

$$\alpha(TCR) = \frac{R_s - R_i}{R_i(T_s - T_i)} \tag{1.3}$$

R_i stands for surface resistance at room temperature, R_s stands for the surface resistance at the last temperature reading, T_s is the last and T_i is the initial temperature.

In this study Lucas Labs Pro 4 FPP system with temperature controller shown in Figure 1.8. is used. Basic measurement accuracy of the equipment is 0.012%.

Figure 1.8. *Lucas Labs Pro 4 FPP system with temperature controller*

1.3.3. Atomic Force Microscopy

AFM is a scanning probe microscopy technique capable of imaging surfaces indirectly down to the atomic level. It is invented by Binnig, Gerber and Quate in 1986 as a tool for surface analysis for both insulator and conductive samples. AFM measures

the deflection of a cantilever (a component the tip is attached on) due to the force of interaction between a specimen surface and a sharp probe tip (typically less than 10 nm in diameter) instead of using electron tunneling current to measure the probe tip to sample surface distance as in STM.

The AFM instrument used in this study is Veeco Nanoscope IV Multimode which is designed for imaging small (approximately 1.5 cm diameter) samples using a series of interchangeable scanners and is able to provide images from the atomic scale to 175 μm in size. As it is described in its user manual, the system is comprised of two main components: the scanner and the AFM detection system. The scanner houses the piezoelectric transducer. The piezo element physically moves the sample in the X, Y and Z direction. The detection system consists of a laser which generates a spot of light that is reflected from a micro cantilever onto a mirror and finally into a photodetector. The position of the spot is determined by the photodiode circuitry. The generated signal is processed by the computer and visualized as a surface image [19].

In this thesis tapping mode AFM is used for measurements. One advantage of tapping mode AFM is an absence of frictional forces which exert torque on the cantilever. The feedback loop keeps a vibrating cantilever at constant amplitude, rather than keeping a cantilever at a constant deflection. The tip on the cantilever is modulated through mechanical excitation at its resonance [19].

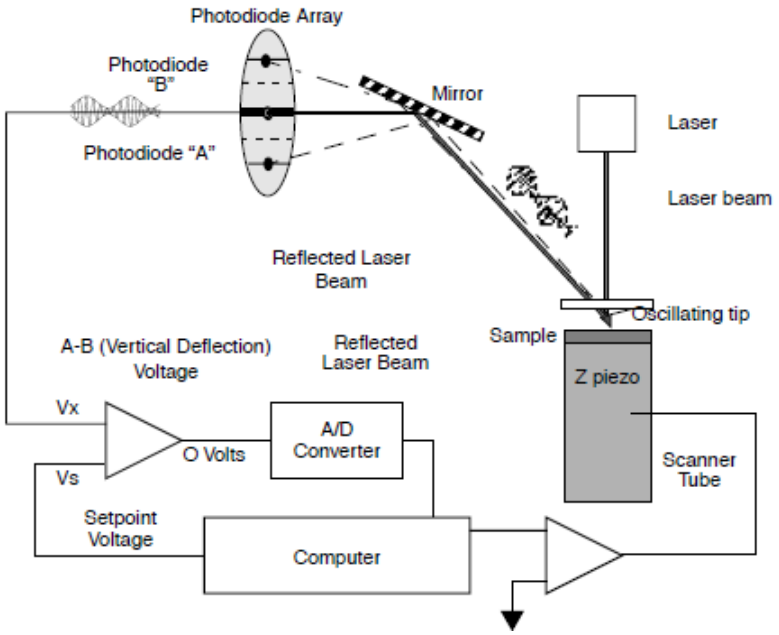

Figure 1.9. *Schematic diagram showing the main components and operating principles of the AFM in tapping mode. [19]*

AFM provides atomic scale vertical resolution, high lateral spatial resolution, imaging of insulating samples and it is possible to obtain magnetic, electrochemical, and hardness properties with special equipment implementation [20].

Figure 1.10. *AFM system at Anadolu University Advanced Technology Thin Film Laboratory*

2. EXPERIMENTAL PROCEDURE

In this section substrate selection and preparation, deposition parameters and characterization techniques are explained. Vanadium oxide thin film deposition is made in UHV Sputtering System with P-DC RMS. Si/Si_3N_4 substrates are preferred. Projected film thickness is approximately 100 nm. 99.9995 % pure oxygen and 99.9999 % pure argon gas is used in sputtering process.

2.1. Preparation of the Sputtering System

Sputtering chambers have to be cleaned after certain limits. Amount of deposition made, and target material changes necessitates cleaning of the parts inside the chamber to maintain a high vacuum, prevent contamination and arc formation. Any debris or chipping formed during previous depositions may cause arcing.

System is carefully cleaned before the experiments to remove remnants of previous depositions and contaminants. All removable parts are washed in ultrasonic bath with high purity ethanol for 20 minutes and carefully dried with 99,999 % nitrogen gas before reassembly. Bake-out procedure at 120°C temperature applied for 48 hours to remove water vapor inside the system and establish a high base vacuum on the order of 10^{-9} Torr.

2.2. Substrate Selection and Coating Thickness Determination

Substrate selection is an important procedure as substrates are the birthplace of all thin films. Nucleation and subsequent growth of the thin film is directly affected by the substrate chemistry and physical properties such as surface roughness. Sputtered thin films are almost always under stress and one of the effective reason for the stress is the thermal expansion coefficient difference between the film and the substrate. And lattice mismatch between the film and the substrate results in increased amount of dislocations and internal stress [21][22].

An appropriate substrate candidate for vanadium oxide is Si/SiO_2 with its VO_2 formation enabling properties [23]. Si based substrates are technologically important as most of the electronics depend on silicon based wafers and vanadium oxide films with best MIT parameters are reported to be grown on Si based substrates [24].

In this study n-type, phosphorus doped, 1-30 ohm-cm resistivity, single 1000 nm thick thermal oxide coated Si <100>, Si/SiO_2, (only for electrical characterization) and 250 nm Si_3N_4 coated Si <100>, Si/Si_3N_4, substrates are used.

As a preparatory work, thin film growth characteristics on the Si/SiO_2 and Si/Si_3N_4 substrates are inspected with AFM imaging. Samples are deposited with 5% to 30% O_2/Ar ratios and at two different thicknesses, 20 nm and 100 nm respectively. All other parameters are kept constant. Details of the deposition parameters for the preparatory study are shown in Table 2.1. and results are shown at section 3.2.1. AFM Results of Substrate Selection Study.

Table 2.1. *Deposition parameters that are kept constant for the preparatory study*

P-DC Power (W)	Target Angle (°)	Base Pressure (Torr)	Thickness (nm)	Duty Cycle (%)	Target to Substrate Distance (mm)	Substrate Rotation (rpm)	Pulse Frequency (kHz)
70	21	$<10^{-8}$	20 & 100	25	50	60	50

2.3. Substrate Preparation

Cleaning substrates is an important process since any contamination on the surface can affect the nucleation and film growth stages. Organic residue, dust particles and remnants of chemicals should be carefully removed from the surface. Substrates must be carefully handled after cleaning to prevent any contamination.

Substrates are sliced into 10 mm to 10 mm square shapes before the cleaning in order to minimize the cost and also to meet with the limitations of characterization equipments such as AFM.

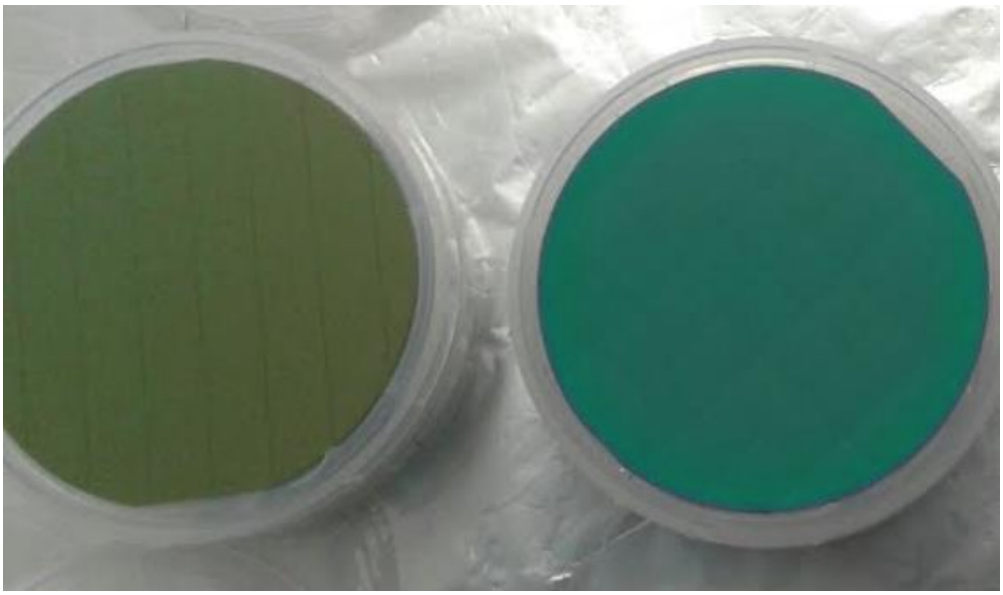

Figure 2.1. *Si/SiO_2 and Si/Si_3N_4 substrates sliced into 10 mm to 10 mm squares*

The cleaning procedure begins with immersing the substrates into 99.5 % pure acetone for 10 minutes, and then they are carefully immersed into 99.8 % purity propanol. After the solvents substrates are rinsed with deionized water and dried with 99.999 % pure nitrogen gas. Cleaned and dried substrates are loaded to special holders that locks the substrates tightly in place and put inside the high vacuum load lock chamber of the sputtering system.

2.4. Deposition Process

Deposition parameters apart from the duty cycle are taken from a previous thesis study conducted in the same sputtering chamber at Anadolu University Advanced Technology Thin Film Laboratory since the results were promising for electrical properties [25]. 99.95 % pure vanadium metal target, 99.9999 % pure Ar and 99.9995 % pure O_2 gases are used. A precleaning deposition with 2 sccm argon gas flow employed after each production cycle to purge the vacuum chamber and clean the target surface. Constant deposition parameters are listed in Table 2.2.

Table 2.2. *Deposition parameters that are kept constant for the experiments*

P-DC Power (W)	Target Angle (°)	Base Pressure (Torr)	Argon Flow (sccm)	Oxygen Flow (sccm)	Deposition Time (s)	Target to Substrate Distance (mm)	Substrate Rotation (rpm)	Pulse Frequency (kHz)
70	21	$<10^{-8}$	2	0.4	2857	50	60	50

2.4.1. Duty Cycle Determination

Pulsed DC (P-DC) power source used in this study, the Advanced Energy Pinnacle Plus+ 5 kW Power Supply, has a micro and hard arc handling feature to protect the system that limits the range of duty cycles available. User manual of the power supply shows 2% to 45% duty cycle is possible for 50 kHz frequency in theory as shown in Table 2.3., but duty cycles that can be used with the chosen deposition parameters found to be between 10% and 32.5% with trials. Below 10% plasma did not form and after 32.5% hard arc observed. As recommended in the user manual, arc trip level is set above 60 V, and no hard arc formed during the deposition processes between 10% and 32.5% duty cycles.

Table 2.3. *Duty Cycle limits for a given self-run frequency [26]*

Requested Frequency (kHz)	Actual Frequency (kHz)	Pulse Reversal Time Maximum (µs)	Duty Cycle (min%) Reverse/ Period	Duty Cycle (max%) Reverse/ Period
35	35.026	10	1.40	35.0
40	40	10	1.60	40.0
45	45.045	9.9	1.80	44.6
50	50	9.0	2.00	45.0
55	54.945	8.1	2.20	44.5

The sputtering system does not allow adjusting the duty cycle directly, it allows changing the pulse duration time (PDT, pulse-on time) at constant pulse frequency (50 kHz). PDT is the actual sputtering duration for each pulse cycle, dielectric surfaces discharge during the pulse-off time as illustrated in Figure 1.3.

Sample depositions started from 10% duty cycle and increased by 5% increments for each subsequent sample up to 30%. Characterization results of samples with duty cycles higher than 20% are found to be of interest in terms of electrical properties. Hence intermediate duty cycle values over 20% are produced with 2.5% increments reaching the highest allowable value of 32.5%. Required PDT values for the deposition processes are calculated by using Equation 1.1. Sample production plan is given in Table 2.4.

Table 2.4. *Sample Production Plan*

Run No	Run Name	P-DC Power (W)	Pulse Frequency (kHz)	PDT (µs)	Duty Cycle (%)
1	VS-204-10-1	70	50	2	10
2	VS-204-15-1	70	50	3	15
3	VS-204-20-1	70	50	4	20
4	VS-204-25-1	70	50	5	25
5	VS-204-30-1	70	50	6	30
6	VS-204-22,5-1	70	50	4.5	22.5
7	VS-204-27,5-1	70	50	5.5	27.5
8	VS-204-32,5-1	70	50	6.5	32.5

2.5. GI-XRD Measurements

For X-ray diffraction analysis Bruker D8 Advance is used. System has Cu-Kα X-ray tube and Brag-Brentano geometry with grazing incidence capability.

In this study GI-XRD technique is used for phase analysis to isolate the signals of the film from the substrate. Height scan conducted on the samples to position the X-rays

on the middle. Appropriate omega angle (ω) is determined by scanning the samples with ω < 1°. X-ray tube is fixed at 1° and the power source is set to 30 mA and 40 kV. Samples are scanned between 10° to 70° with 0.05° steps.

2.6. AFM Measurements

Atomic Force Microscopy is used to measure the grain size and surface roughness and to visualize the film surface. Effect of duty cycle on grain size and surface roughness checked.

The AFM system used for this study is Veeco NanoScope IV Multimode. Tapping mode AFM and data analysis software Bruker NanoScope Analysis v. 1.5 is preferred.

Type of tapping mode AFM tip used is Bruker RTESP MPP-11100-10. The tip has rotated (symmetric) geometry and supports resonant frequency from 200 to 400 kHz, spring constant from 20 to 80 N/m. Nominal tip radius is 8 nm and cantilever material is Sb (n) doped Si with 0.01-0.025 Ωcm resistance.

2.7. FPP Measurements

FPP measurements are conducted using computer controlled Lucas Labs Pro4-4000 FPP system with Keithley 2400 power source. Distance between the probes is 1.016 mm. Osmium alloy probes are used instead of more common tungsten carbide types since they are softer and provide more stable contact without damaging the film.

Sheet resistance and resistivity are calculated automatically by the computer. Only geometrical dimensions and the film thickness are provided to the software by the operator. Appropriate current value is determined by the computer through applying different currents to the sample.

Resistance change with respect to temperature is measured manually by implementing an uncooled hot plate with electronic control unit under the sample and a portable thermocouple touching on the sample surface. Resistance, resistivity and sample surface temperature values are recorded for each 5°C increase in the hot plate starting from room temperature and reaching up to 120°C. TCR values are calculated and graphed by using OriginPro 8 software.

3. RESULTS AND DISCUSSION

In order to determine the coating thickness and O_2/Ar ratio for sputtering a preparatory substrate selection study is conducted by depositing 20 samples. 20 nm and 100 nm thick coatings are deposited onto Si/SiO_2 and Si/Si_3N_4 substrates with 5 different O_2/Ar rates ranging from 5% to 30%.

To see the effect of duty cycle on vanadium oxide thin films deposited by P-DC RMS technique 16 samples are produced at 8 deposition cycles with different duty cycle values. Duty cycle increment for the first experiment is 5% starting from 10% and ending at 30%. Second experiment is conducted to increase the resolution of results since the sample with 25% duty cycle showed interesting properties. It is the only sample that shows a vanadium oxide crystallization in GI-XRD results.

Two different substrates are loaded for each deposition cycle, one Si/SiO_2 and one Si/Si_3N_4. Samples with Si/SiO_2 substrates are only used for electrical characterization.

List of samples and deposition parameters are given in Table 3.1 and Table 3.2.

Table 3.1. *List of deposited samples & deposition parameters for 1st experiment*

Run Name	Sample Name	Duty Cycle (%)	PDT & Pulse Frequency (μs & kHz)	P-DC Power (W)	Base Pressure (Torr)	Ar & O_2 Flow Rate (sccm)
VS-204-10-1	VS-204-10-Si	10	2 & 50	70	4.8×10^{-9}	2 Ar 0.4 O_2
	VS-204-10-SiN					
VS-204-15-1	VS-204-15-Si	15	3 & 50	70	1.6×10^{-9}	2 Ar 0.4 O_2
	VS-204-15-SiN					
VS-204-20-1	VS-204-20-Si	20	4 & 50	70	6.0×10^{-9}	2 Ar 0.4 O_2
	VS-204-20-SiN					
VS-204-25-1	VS-204-25-Si	25	5 & 50	70	4.0×10^{-9}	2 Ar 0.4 O_2
	VS-204-25-SiN					
VS-204-30-1	VS-204-30-Si	30	6 & 50	70	6.5×10^{-9}	2 Ar 0.4 O_2
	VS-204-30-SiN					

Table 3.2. *List of deposited samples & deposition parameters for 2nd experiment*

Run Name	Sample Name	Duty Cycle (%)	PDT & Pulse Frequency (µs & kHz)	P-DC Power (W)	Base Pressure (Torr)	Ar & O_2 Flow Rate (sccm)
VS-204-22.5-1	VS-204-22.5-Si	22.5	2 & 50	70	6.7×10^{-9}	2 Ar 0.4 O_2
	VS-204-22.5-SiN					
VS-204-27.5-1	VS-204-27.5-Si	27.5	3 & 50	70	4.5×10^{-9}	2 Ar 0.4 O_2
	VS-204-27.5-SiN					
VS-204-32.5-1	VS-204-32.5-Si	32.5	4 & 50	70	5.2×10^{-9}	2 Ar 0.4 O_2
	VS-204-32.5-SiN					

All deposition pressures were stable at 3.2×10^{-3} Torr and no hard arc formation detected.

3.1. GI-XRD and TEM Results

Phase analysis with GI-XRD technique conducted on samples deposited on Si/Si_3N_4 substrates. Samples are scanned between 10° to 70° with 0.05° steps (40 seconds for each step) at 30 mA and 40 kV. Results are given at Figure 3.1.

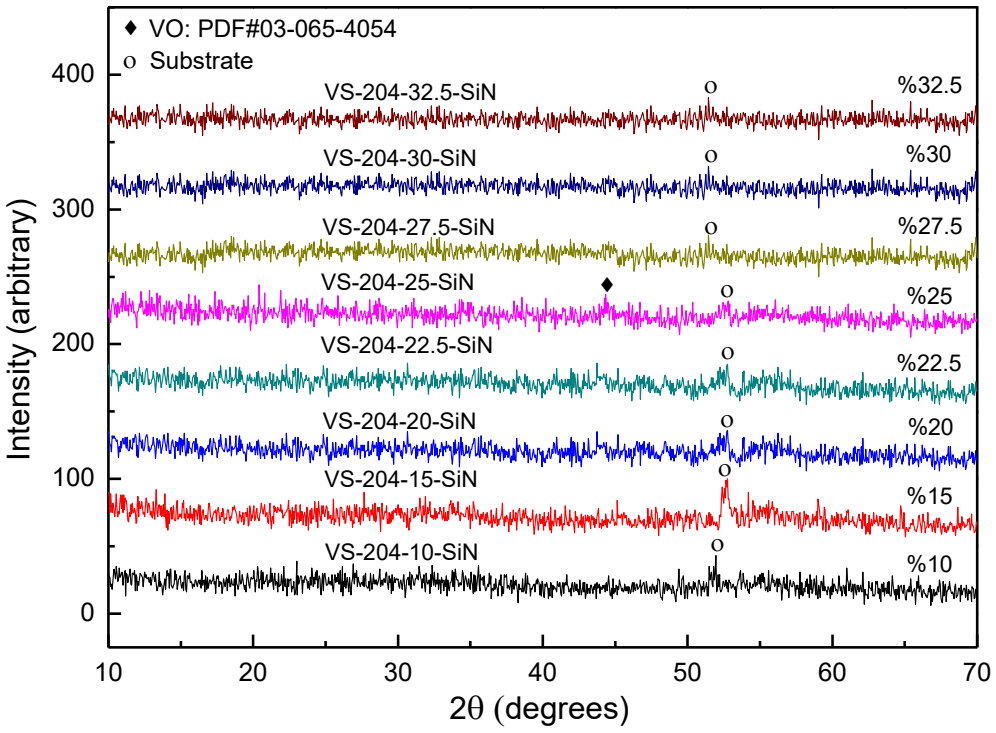

Figure 3.1. *GI-XRD results of samples deposited on Si/Si_3N_4 substrates at different duty cycle values. Duty cycle values are shown at right side.*

GI-XRD analysis of the deposited films showed amorphous structure except for the sample VS-204-25-SiN produced with 25% duty cycle. In this sample VO crystallization observed which may indicate nanocrystalline structure.

Dark field and bright field TEM imaging studies carried out on the VS-204-25-SiN at Bilkent University National Nanotechnology Research Center (UNAM) in order to confirm the VO crystallization seen in GI-XRD results. Results confirmed the finding as seen in Figure 3.2. Dark regions in bright field image and light regions in dark field image indicate nanoscale vanadium oxide crystals.

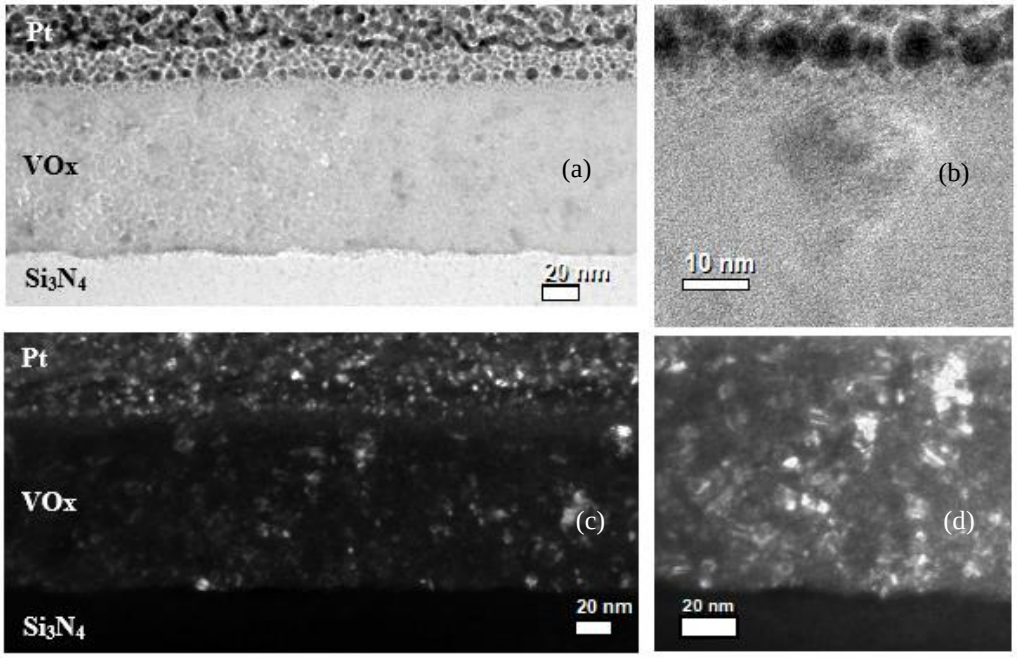

Figure 3.2. *TEM images of the sample deposited with 25% duty cycle. Vanadium oxide crystals are seen throughout the film as high contrast regions. (a) Bright Field Image, (b) High Magnification BF Image, (c) Dark Field Image, (d) High Magnification Dark Field Image.*

3.2. AFM Results

Substrate selection study samples are analyzed at AFM right after deposition process to decrease the effect of surface deterioration resulting from exposure to ambient air. Duty cycle samples are analyzed after GI-XRD measurements since risk of contamination during AFM measurements may affect the GI-XRD results.

All samples are scanned with tapping mode at 0° angle and 1.969 Hz scan rate. 1μm to 1μm scan size with 512 sampling rate and 30 nm data scale is used. Average grain size and surface roughness values are measured using original software provided by the

manufacturer of the AFM equipment, Bruker, NanoScope III version 5.33R1. Error bars on graphs of all samples are taken from the error values shown by the equipment, and they indicate an average of 95% confidence interval. Error bars of the substrate measurements are calculated from standard deviation between the measurements.

3.2.1. AFM Results of Substrate Selection Study

For substrate selection samples are deposited on Si/SiO_2 and Si/Si_3N_4 substrates with parameters given at Table 2.1. Also 5 different O_2/Ar ratios are used to observe the change in average grain size and surface roughness. Grain size and surface roughness of the substrates are measured before deposition as reference values and averages shown in graphs as 0% O_2/Ar ratio, given in Figure 3.3. and 3.4.

In terms of surface roughness, 20 nm thick samples deposited on Si/SiO_2 substrates show a considerable increase at 5% and 10% O_2/Ar ratios and continue in a relatively flat trend after 10%. On the other hand, 20 nm thick samples deposited on Si/Si_3N_4 substrates show considerable increase at 20% O_2/Ar ratio. In 100 nm thick samples, regardless of the substrate used, the highest surface roughness is observed at 5% O_2/Ar ratio. Above 5% O_2/Ar ratio roughness decreases and stays at relatively similar values. It can be concluded that above 5% O_2/Ar ratio thin film growth mode changes from layer plus island type (Stranski-Krastanov type) to layer by layer type (Frank-van der Merwe type). Result are shown in Figure 3.3.

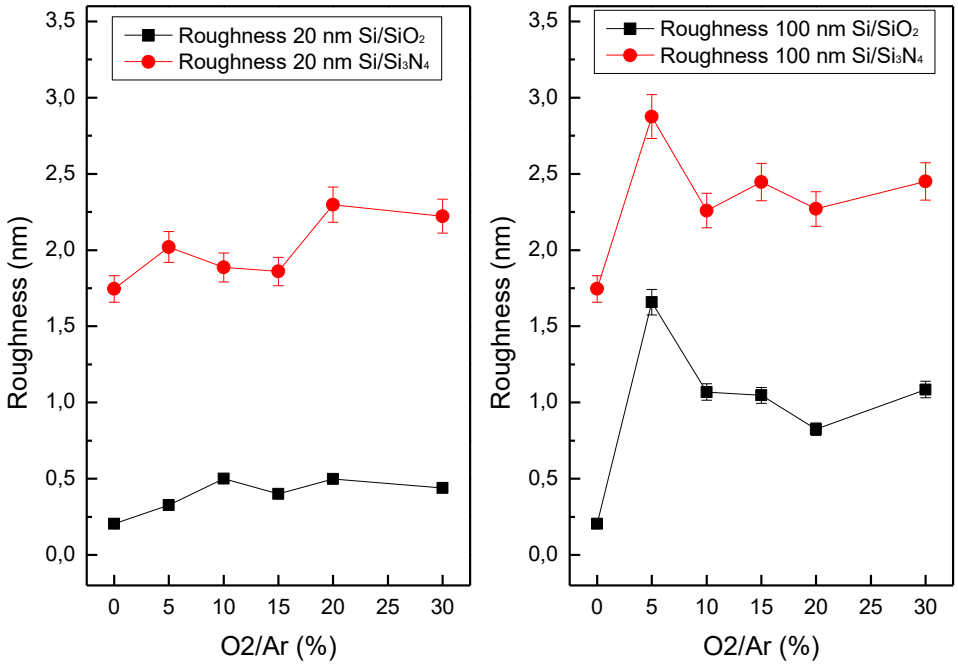

Figure 3.3. *Effect of O_2/Ar ratio, coating thickness and substrate type on surface roughness*

In terms of grain size, only 100 nm thick samples deposited on Si/Si_3N_4 substrates show a controllable increase. This increasing trend may indicate a more uniform film coverage on substrate and Frank-van der Merwe growth type. It is not possible to deduce a correlation for other samples in a confident way.

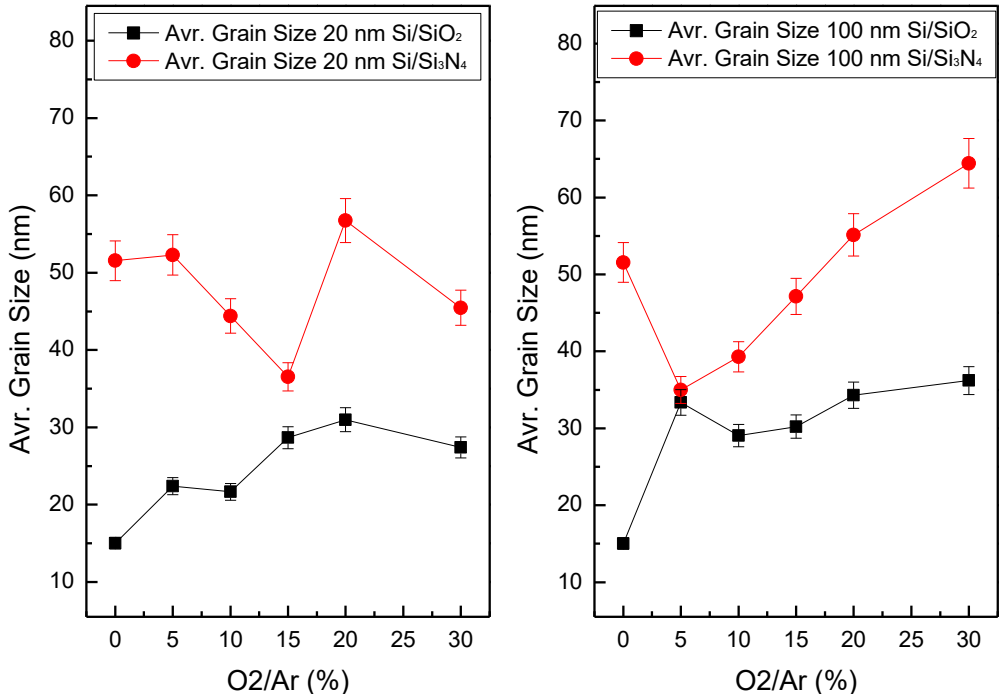

Figure 3.4. *Effect of O_2/Ar ratio, coating thickness and substrate type on average grain size*

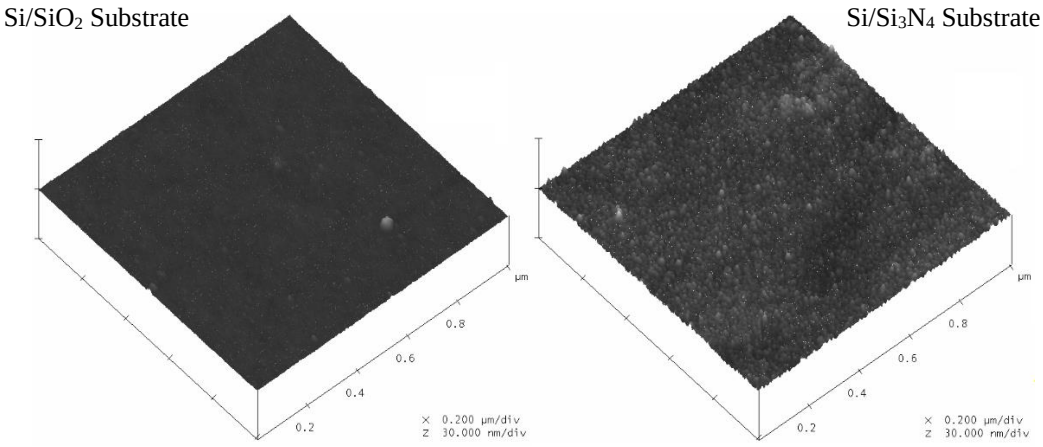

Figure 3.5. *AFM images of samples deposited on Si/SiO_2 and Si_3N_4 substrates with different O_2/Ar ratios*

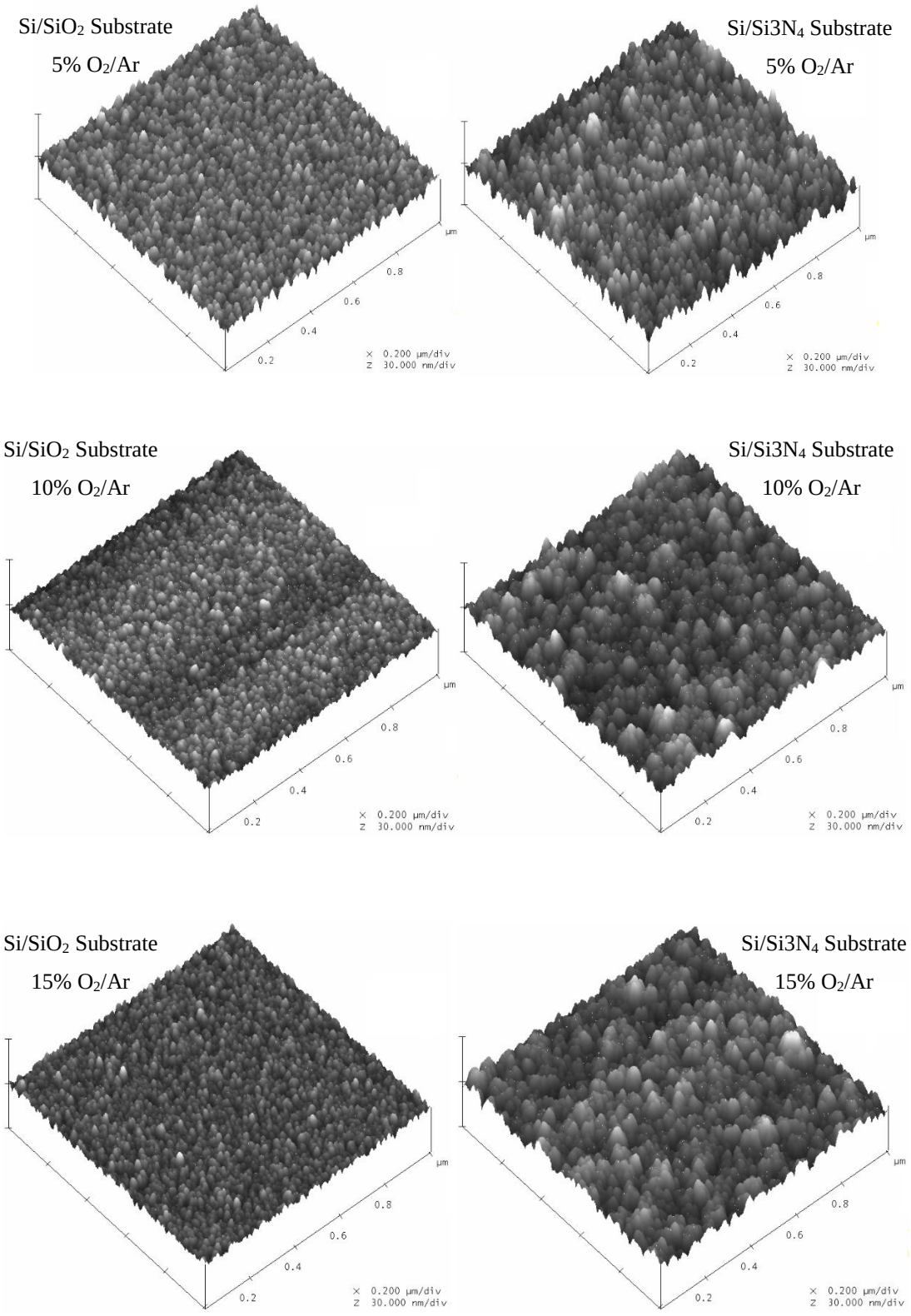

Figure 3.5. *(Continued) AFM images of samples deposited on Si/SiO_2 and Si_3N_4 substrates with different O_2/Ar ratios.*

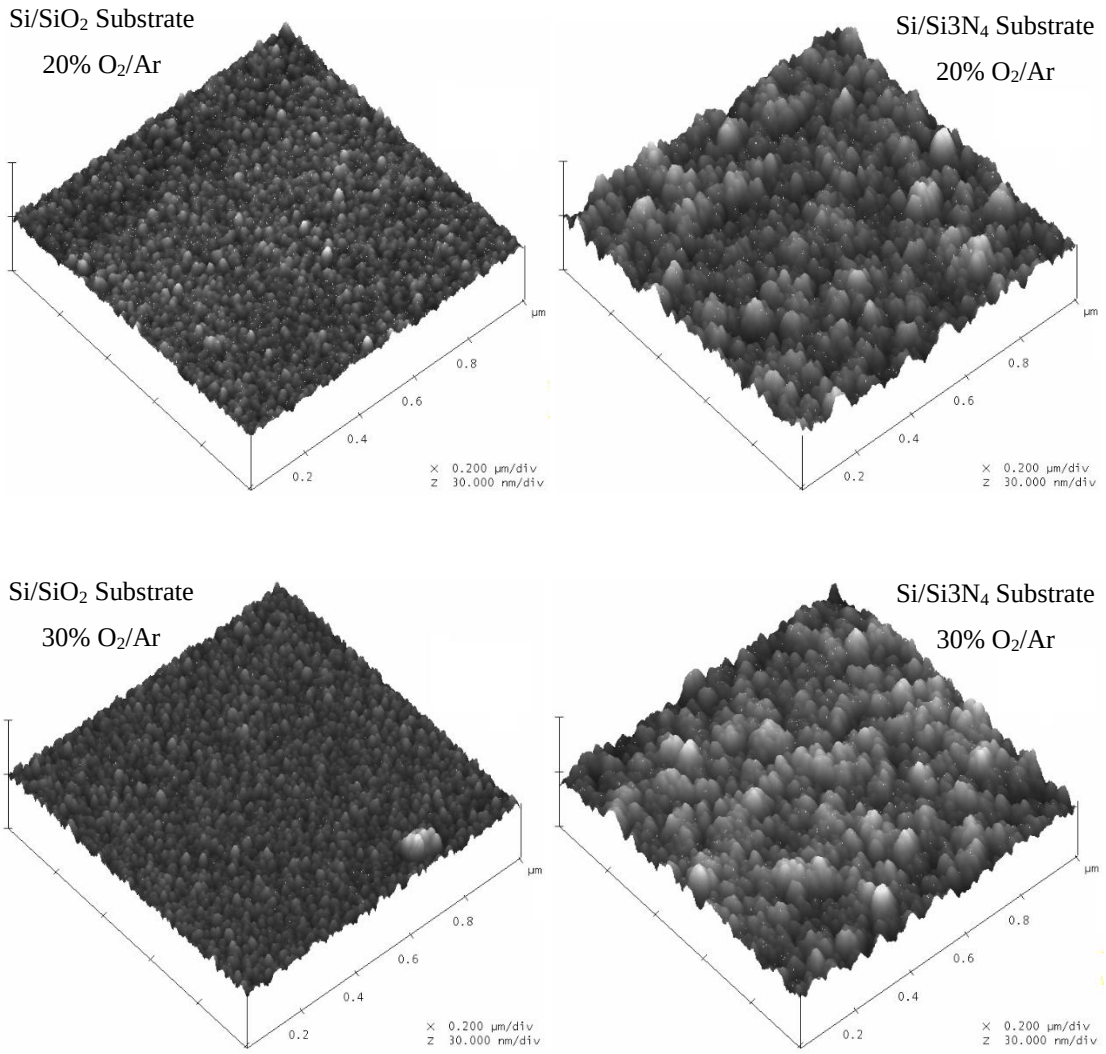

Figure 3.5. *(Continued) AFM images of samples deposited on Si/SiO_2 and Si_3N_4 substrates with different O_2/Ar ratios.*

Comparative analysis results shown in Figure 3.3. and 3.4. suggest that 100 nm coating thickness and Si/Si_3N_4 substrates are more convenient for the study since increasing grain size with relatively steady surface roughness indicates a more uniform growth.

3.2.2. AFM Results of Samples with Different Duty Cycle Values

Results indicate that there is no correlation between the duty cycle and average grain size but mean surface roughness (Ra) shows an inverse proportionality. This decreasing trend in surface roughness values may indicate an increase in structural uniformity with increasing duty cycle. Results are given at Table 3.3. and illustrated with a graph showing the general trend at Figure 3.6.

Table 3.3. *AFM measurement results of samples deposited on Si/Si_3N_4 substrates*

Sample Name	Duty Cycle (%)	Average Grain Size (nm)	Error (± nm)	Mean Roughness (Ra) (nm)	Error (± nm)	RMS Roughness (nm)
VS-204-10-SiN	10.0	60.263	3.0132	1.718	0.0859	2.172
VS-204-15-SiN	15.0	53.155	1.5947	1.658	0.0663	2.097
VS-204-20-SiN	20.0	54.423	1.0885	1.534	0.0614	1.948
VS-204-25-SiN	22.5	35.514	1.4206	1.451	0.0726	1.847
VS-204-30-SiN	25.0	60.183	3.0092	1.546	0.0155	1.963
VS-204-22.5-SiN	27.5	42.670	2.1335	1.584	0.0317	2.029
VS-204-27.5-SiN	30.0	51.454	2.0582	1.364	0.0682	1.742
VS-204-32.5-SiN	32.5	53.266	2.6633	1.498	0.0749	1.901

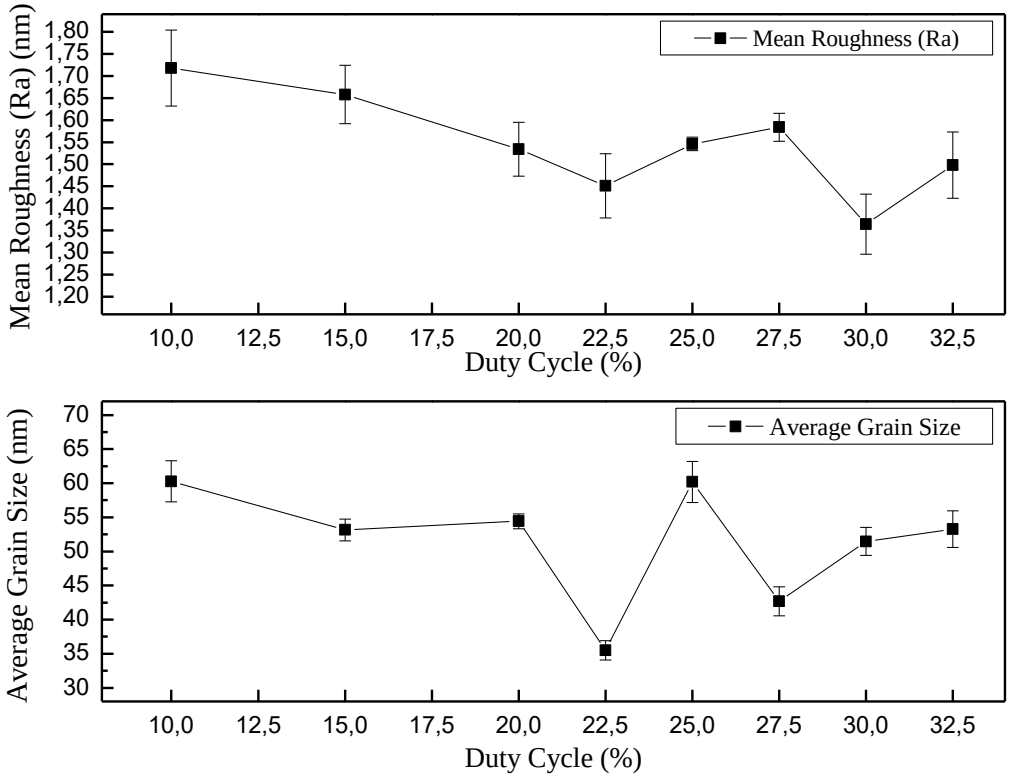

Figure 3.6. *Mean roughness (Ra) and average grain size versus duty cycle*

Three-dimensional AFM images of the samples grown on Si/Si_3N_4 substrates are shown in Figure 3.4. The sample sputtered with 25% duty cycle features an increased amount of fine grains although analysis shows a higher average grain size than others. This may indicate a stronger Stranski-Krastanov growth mode in the sample. As it is seen

in the results there is no correlation between average grain size and duty cycle but certain duty cycles may propagate grain growth whereas others may hinder it.

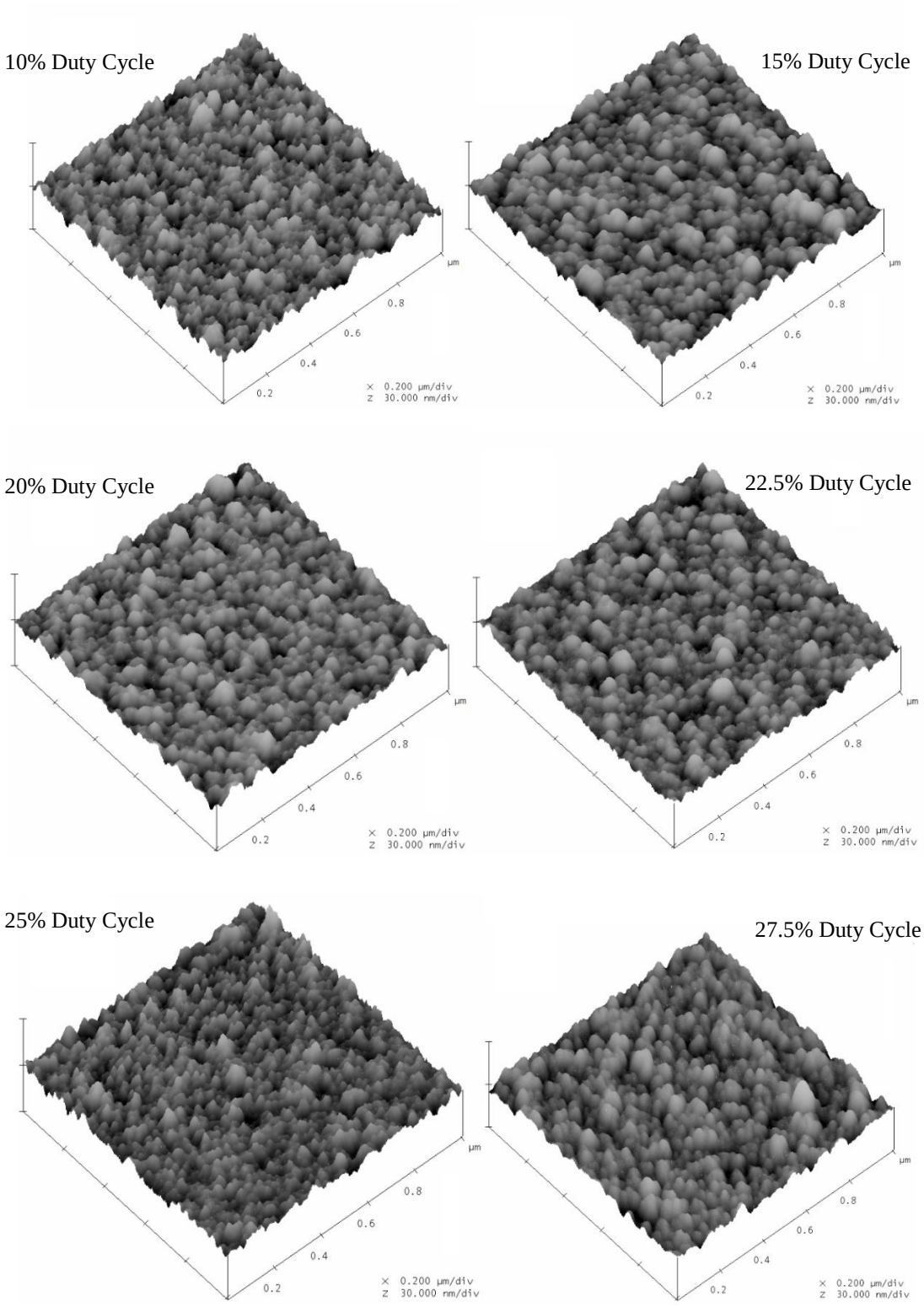

Figure 3.7. *Three-dimensional AFM images of samples deposited with different duty cycle values*

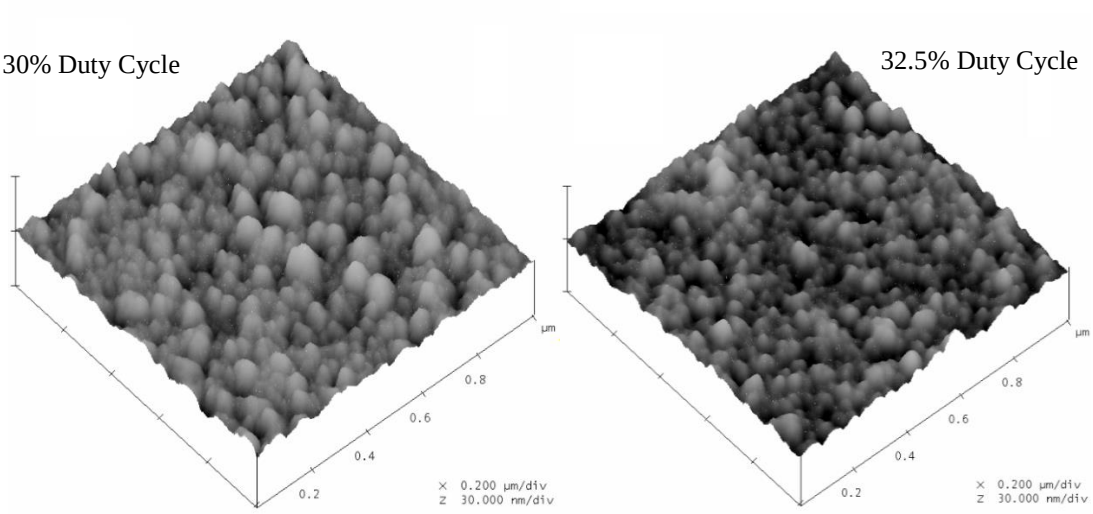

Figure 3.7. *(Continued) Three-dimensional AFM images of samples deposited with different duty cycle values*

3.3. FPP Results

FPP result show an inverse proportionality between the duty cycle and electrical properties of the films. Both sheet resistance and resistivity decreased with increasing duty cycle as shown in Figure 3.5 and Figure 3.6. This characteristic may be attributed to the decreasing porosity and defects in the sample which can be deduced from the regressive trend seen in surface roughness measurements with AFM. Electrical property measurement results are given in Table 3.4.

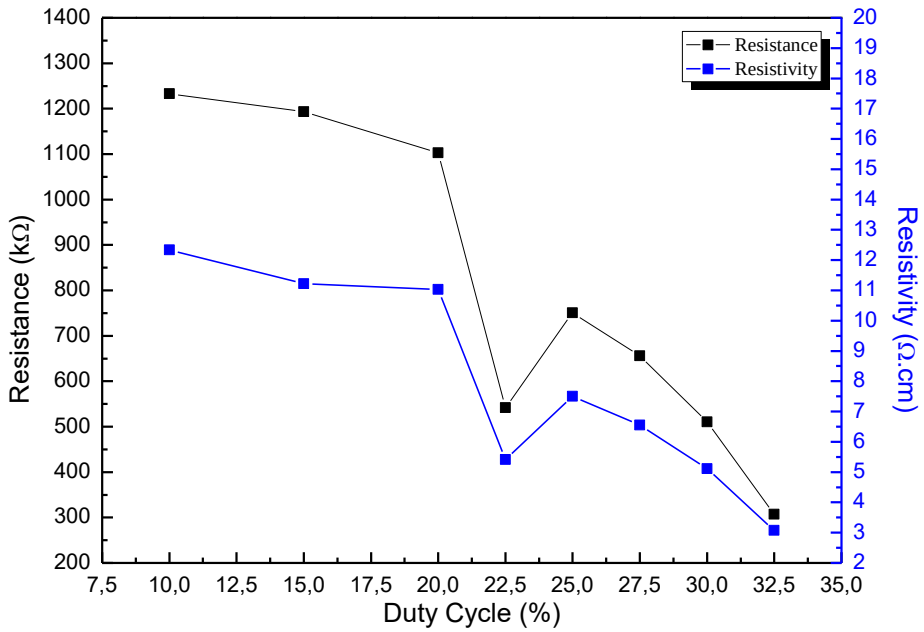

Figure 3.8. *Effect of duty cycle on resistance and resistivity of films on SiO_2 substrates*

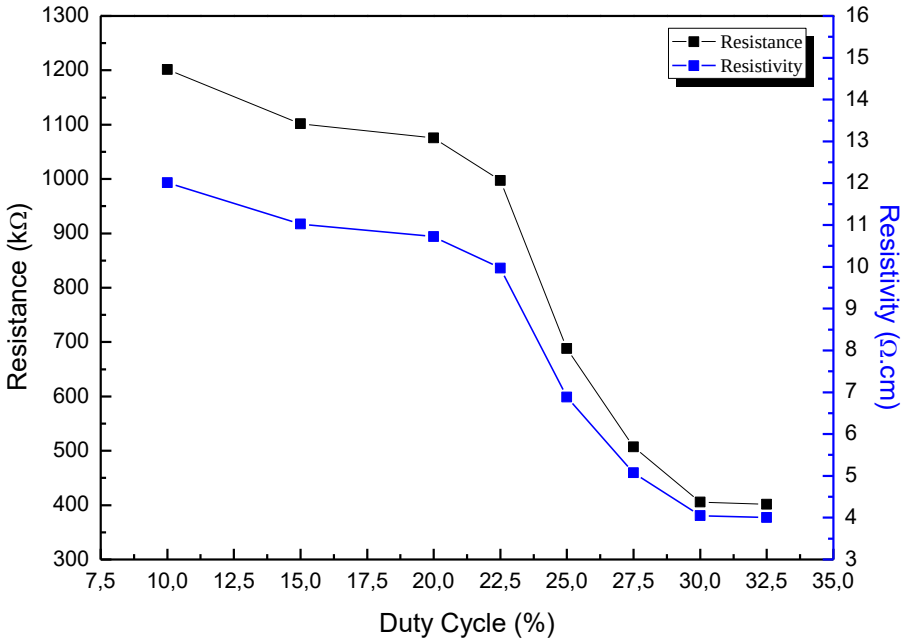

Figure 3.9. *Duty cycle versus resistance and resistivity of films with Si_3N_4 substrates*

Table 3.4. *FPP measurement results. Some TCR measurements failed due to high electrical noise. Basic measurement accuracy is 0.012%*

Sample Name	Duty Cycle (%)	Resistance (kΩ)	Resistivity (Ω.cm)	V (mV)	TCR (-%/°C) Heating/Cooling	
VS-204-10-Si	10	1201.366	12.0137	-13.50	-4.800	-3.852
VS-204-10-SiN		1233.217	12.3322	-14.15	-3.619	-3.279
VS-204-15-Si	15	1101.521	11.0200	-10.01	*Fail*	*Fail*
VS-204-15-SiN		1193.523	11.2170	-12.10	-4.584	-3.926
VS-204-20-Si	20	1075.257	10.7210	-8.54	-0.345	-0.247
VS-204-20-SiN		1102.498	11.0311	-11.01	-0.231	-0.304
VS-204-22.5-Si	22.5	997.230	9.9670	-11.01	-0.404	-0.430
VS-204-22.5-SiN		541.920	5.4100	-7.10	-0.395	-0.360
VS-204-25-Si	25	688.010	6.8800	-8.02	-0.380	-0.417
VS-204-25-SiN		750.326	7.5033	-4.11	-0.261	-0.171
VS-204-27.5-Si	27.5	507.290	5.0700	-2.01	-0.359	-0.257
VS-204-27.5-SiN		656.140	6.5500	-3.40	-0.192	-0.266
VS-204-30-Si	30	405.460	4.0500	-2.07	-0.192	-0.134
VS-204-30-SiN		510.570	5.1100	-2.32	-0.187	-0.137
VS-204-32,5-Si	32.5	401.320	4.0001	-2.10	-3.979	-3.498
VS-204-32,5-SiN		307.190	3.0800	-2.54	*Fail*	*Fail*

For TCR calculations samples are heated from room temperature up to 95°C. Data collected in both heating and cooling cycles with 5°C steps of the heater. High electrical

noise observed in most of the samples during the measurements and results do not show a continuous proportionality. The sample deposited with the highest duty cycle gave a TCR value as high as the lowest duty cycle. There is also an abrupt change in duty cycles over 15%, TCR values of samples with duty cycles higher than this value dropped tenfold and continued at a relatively flat line until 32.5% duty cycle. Also, TCR measurements of two samples, one at high duty cycle and one at low, were unsuccessful due to high voltage fluctuations during heating and cooling cycles resulting in inconsistent readings.

Another observation on TCR measurements is the difference in values between heating and cooling cycles. Readings during cooling were more consistent in general and there is a relatively coherent difference between the values at similar sample temperatures. Heating the samples up to 95°C showed a recovery in electrical noise during cooling. This finding points out the necessity of annealing procedures after deposition. Graphs showing change in R and lnR with respect to temperature are shown in Figure 3.10.

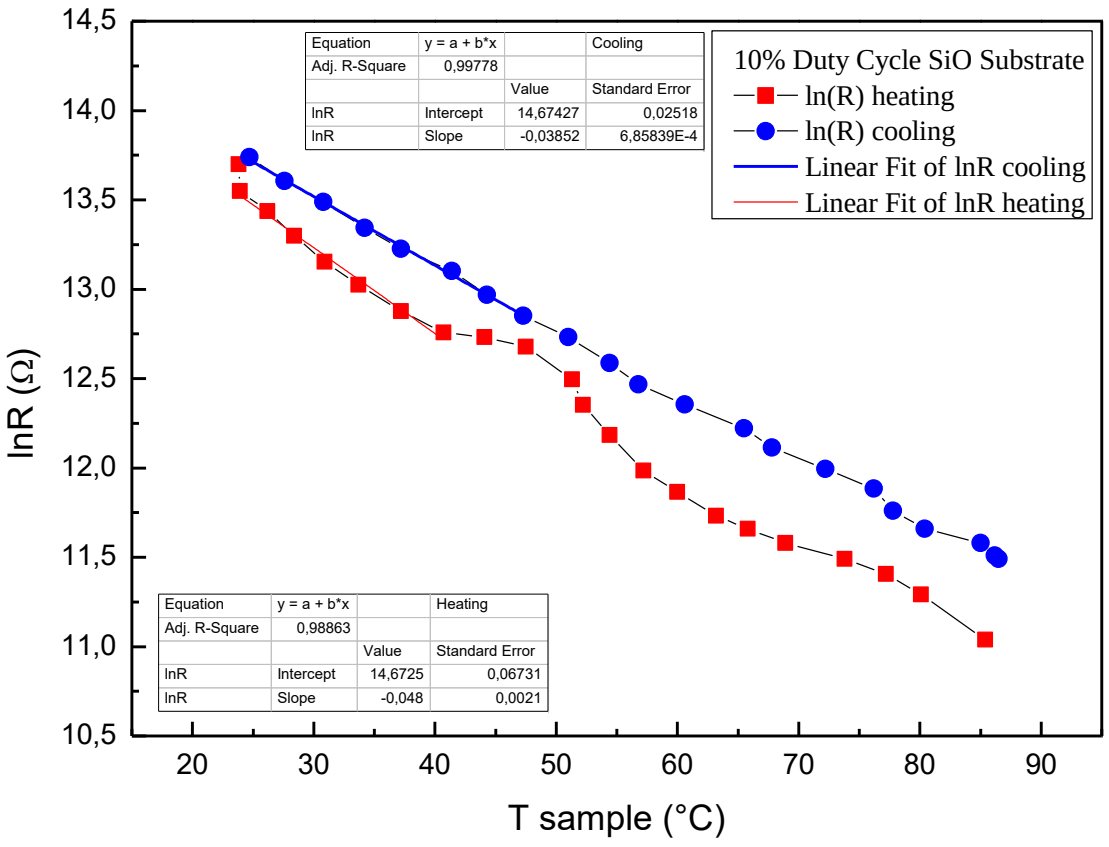

Figure 3.10. *Change in lnR and R with respect to temperature for different samples deposited using duty cycle values*

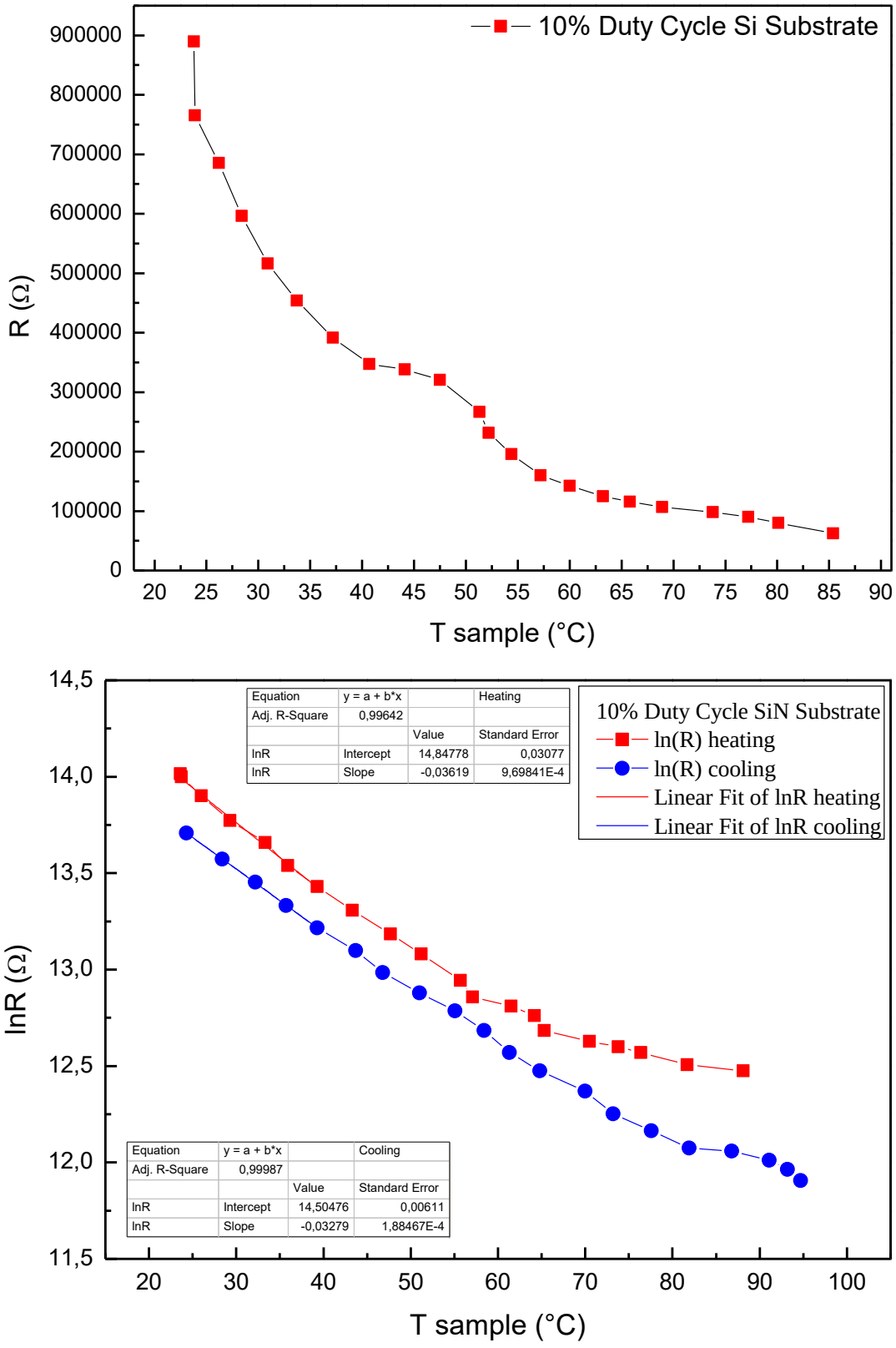

Figure 3.10. *(Continued) Change in lnR and R with respect to temperature for different samples deposited using duty cycle values*

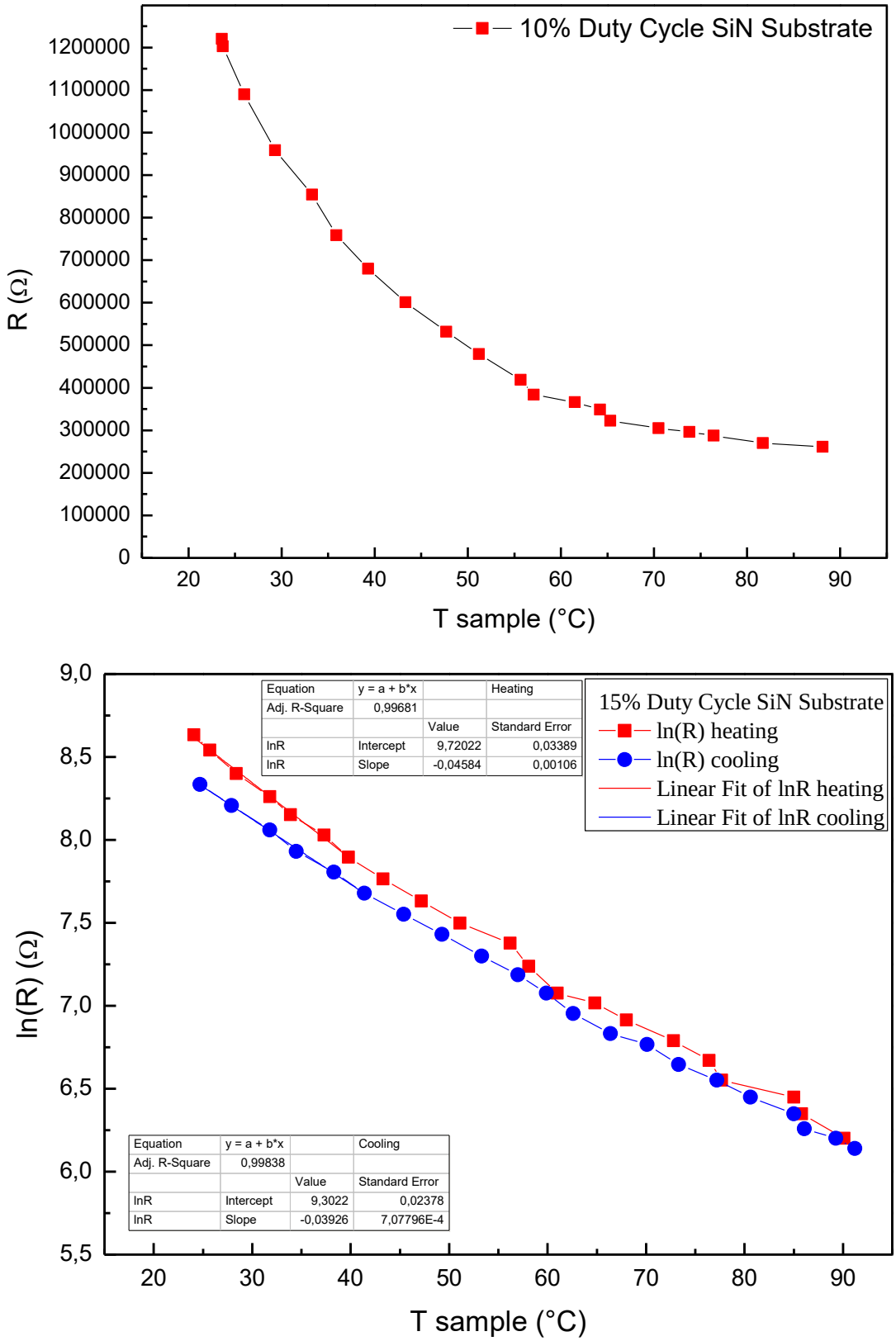

Figure 3.10. *(Continued) Change in lnR and R with respect to temperature for different samples deposited using duty cycle values*

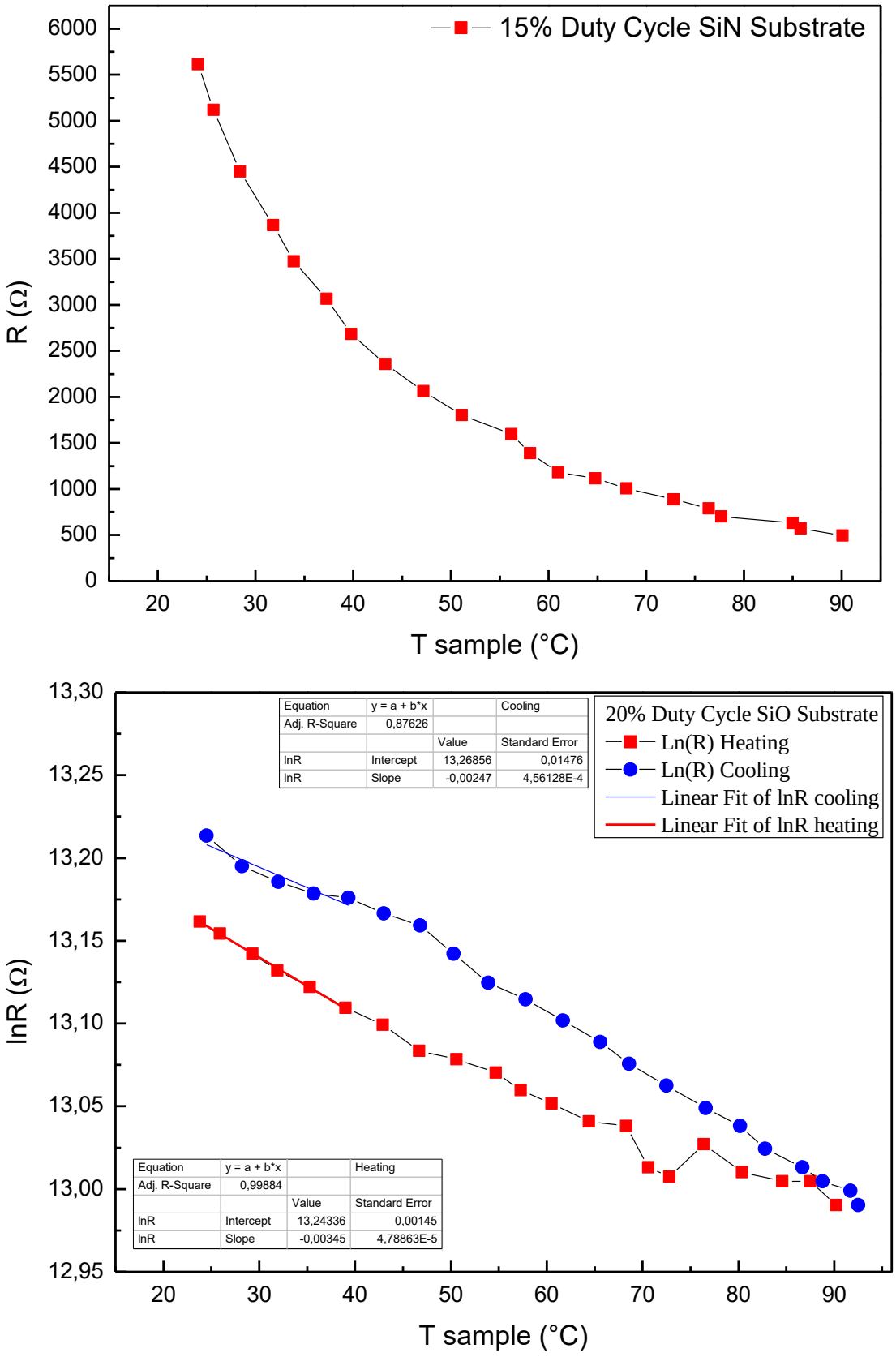

Figure 3.10. *(Continued) Change in lnR and R with respect to temperature for different samples deposited using duty cycle values*

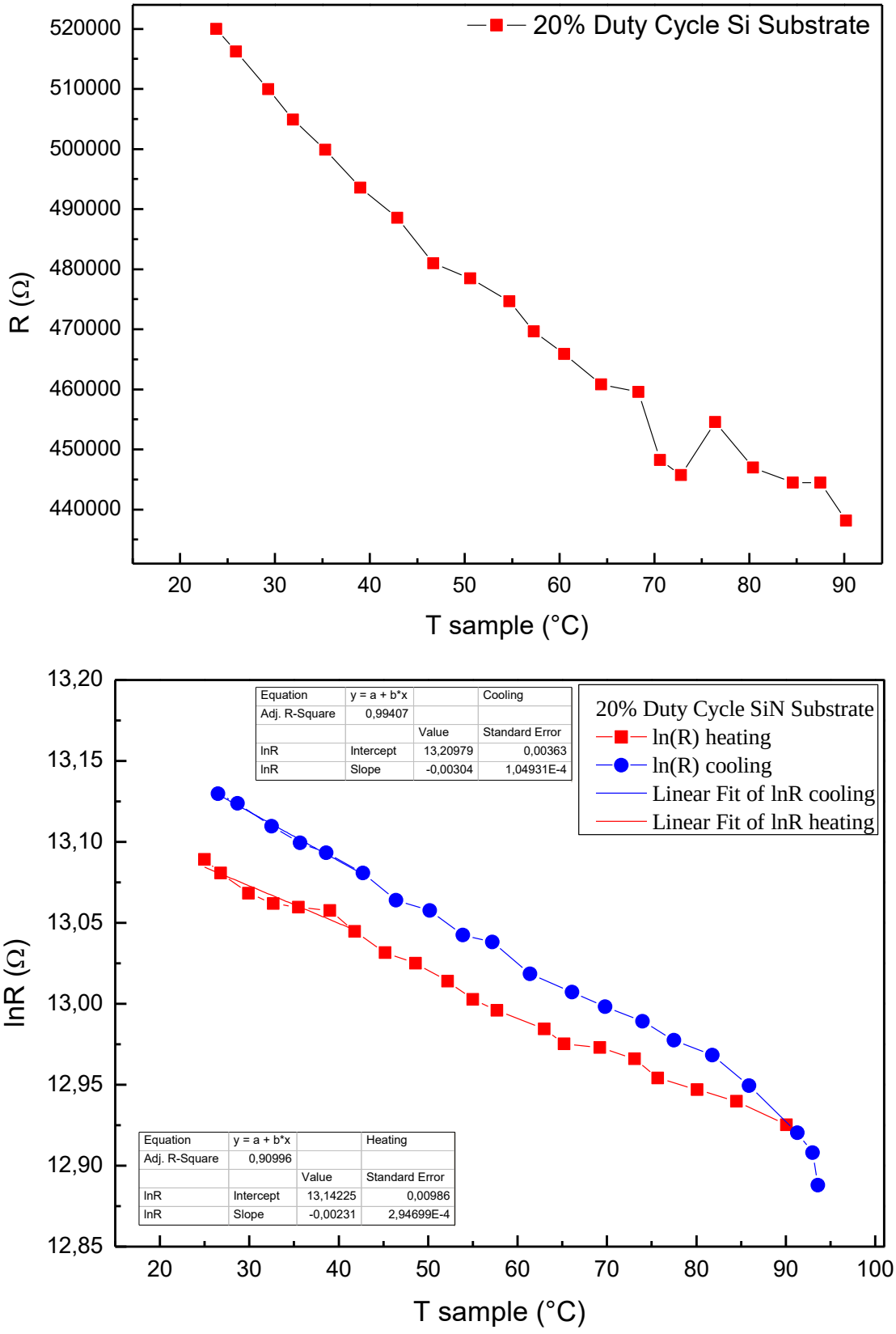

Figure 3.10. *(Continued) Change in lnR and R with respect to temperature for different samples deposited using duty cycle values*

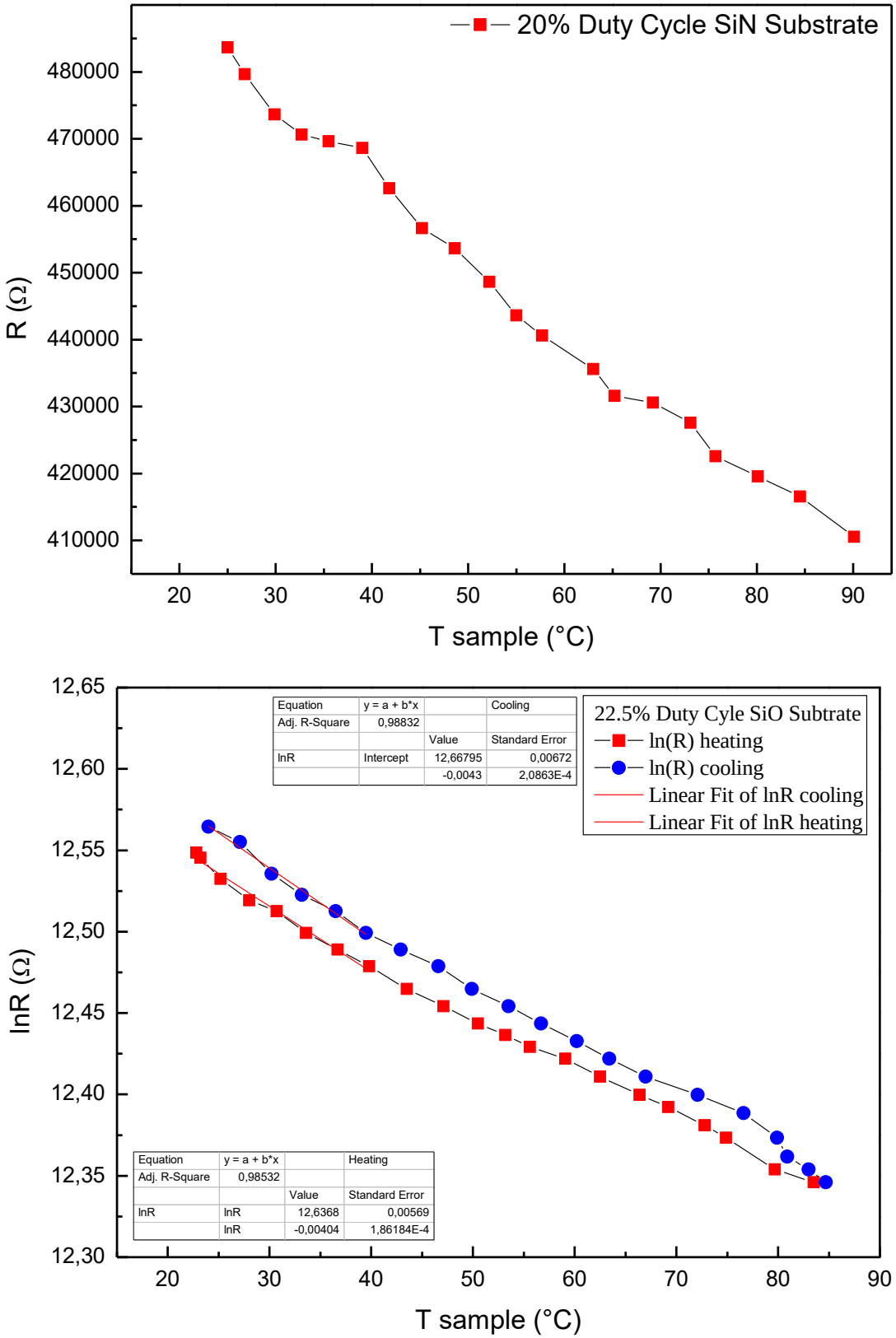

Figure 3.10. *(Continued) Change in lnR and R with respect to temperature for different samples deposited using duty cycle values*

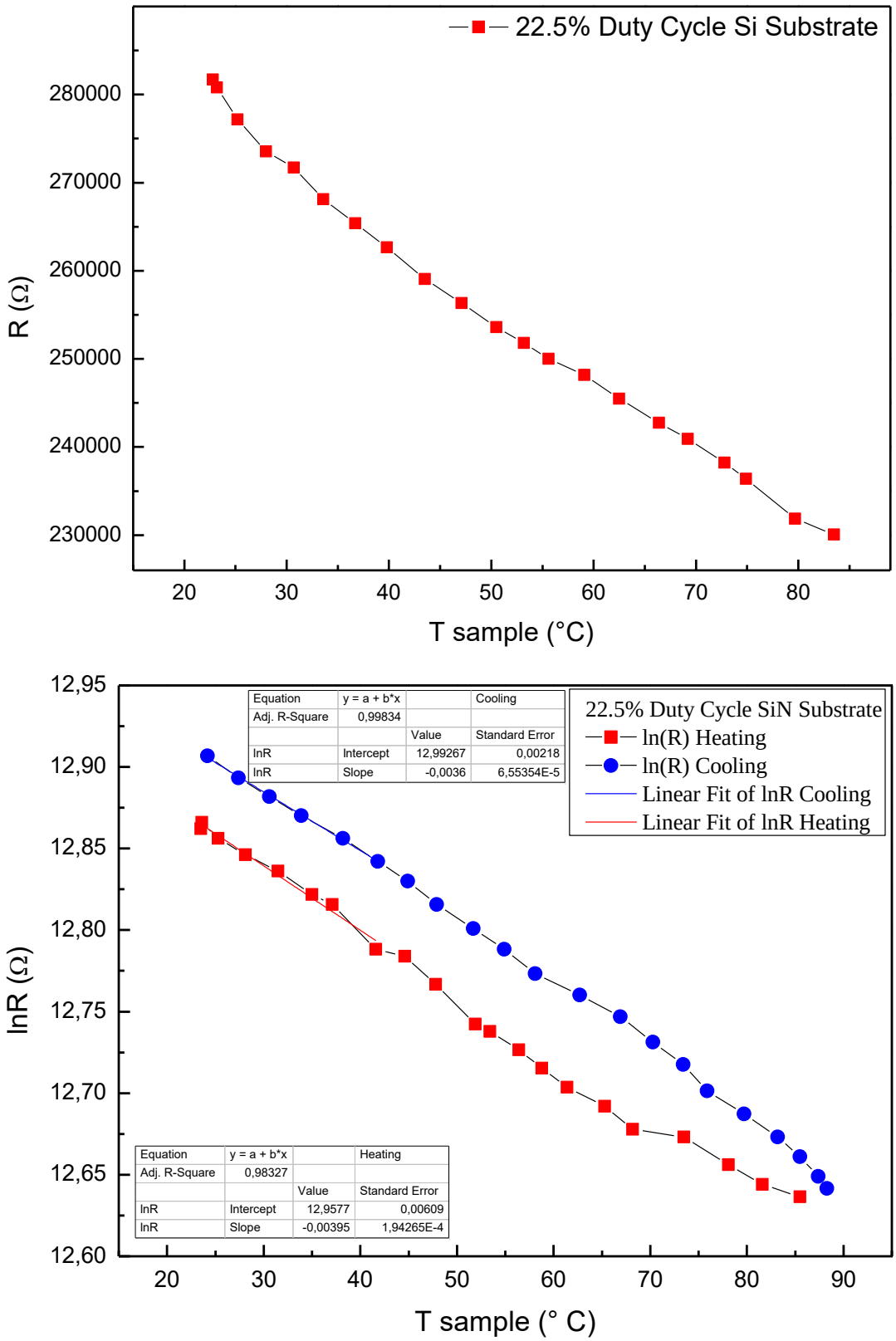

Figure 3.10. *(Continued) Change in lnR and R with respect to temperature for different samples deposited using duty cycle values*

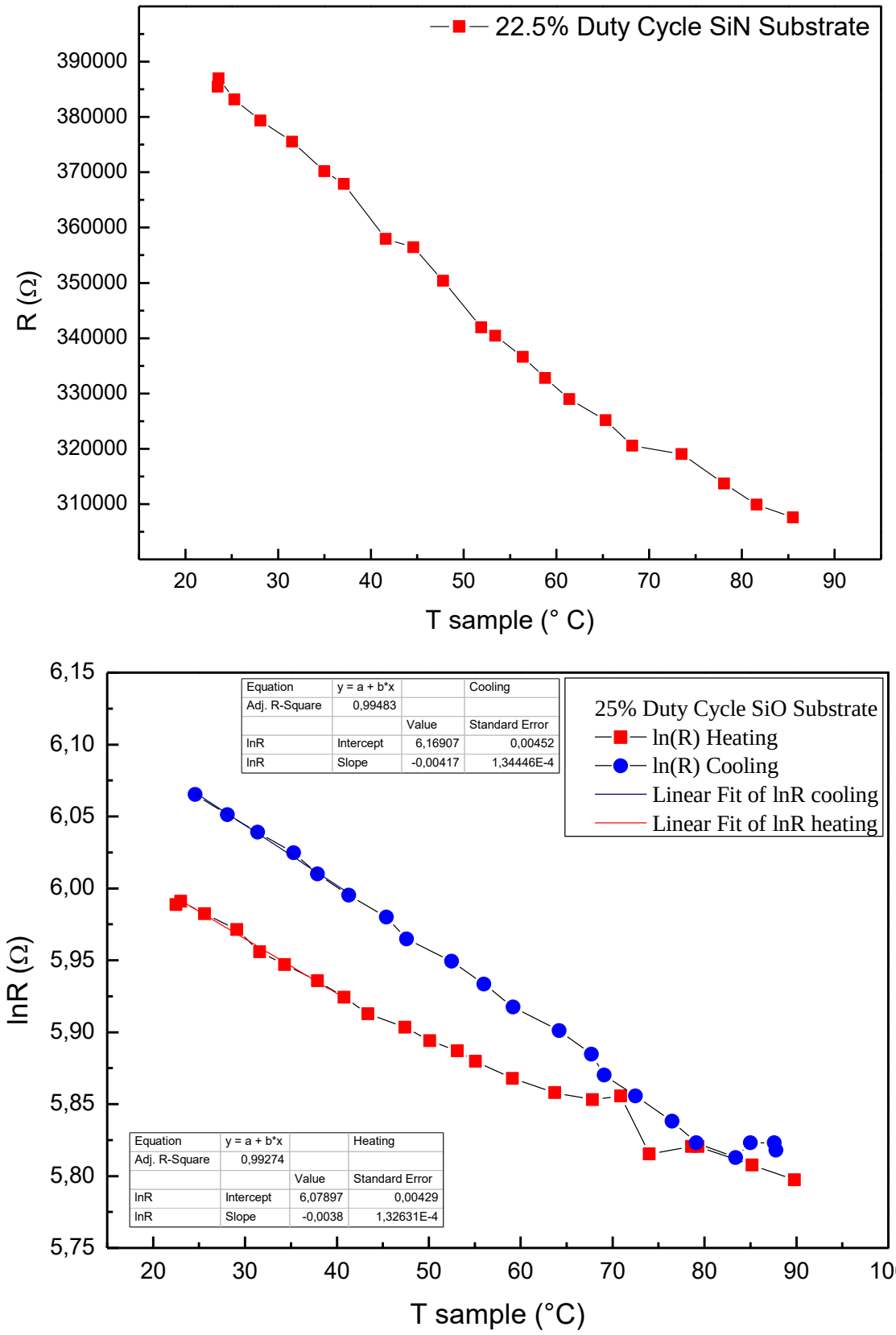

Figure 3.10. *(Continued) Change in lnR and R with respect to temperature for different samples deposited using duty cycle values*

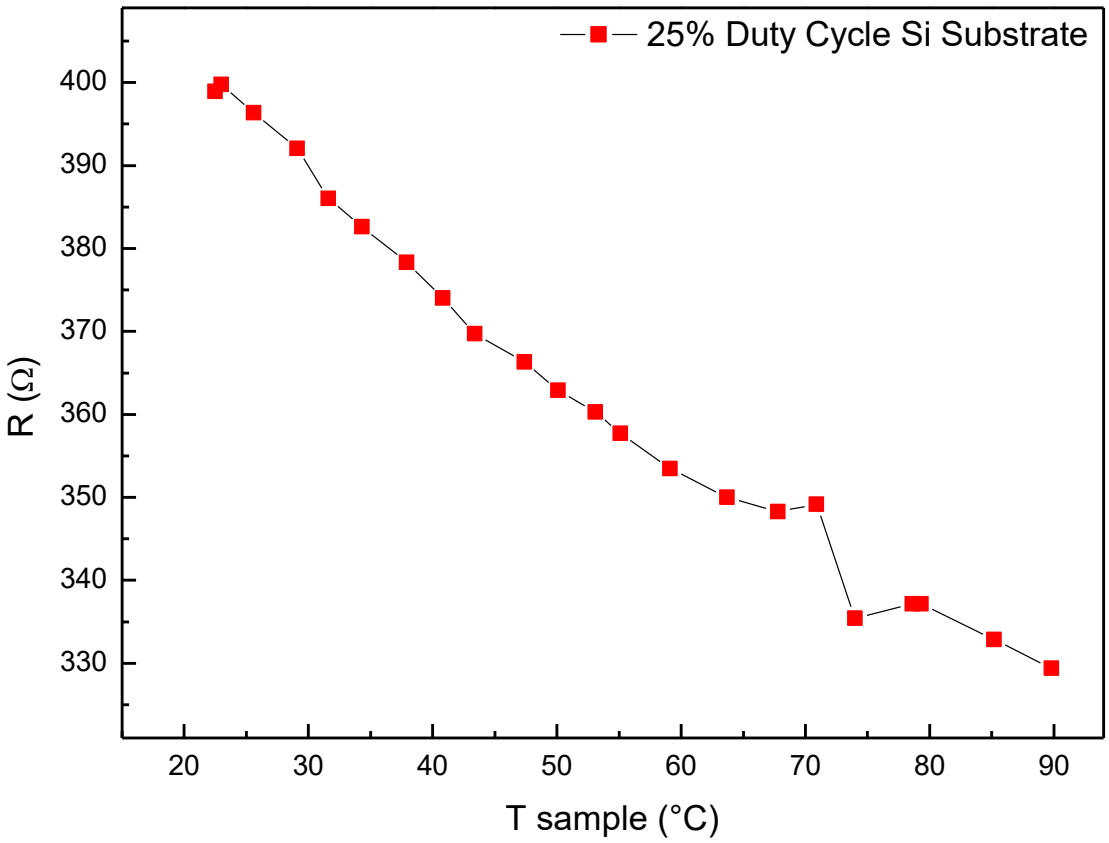

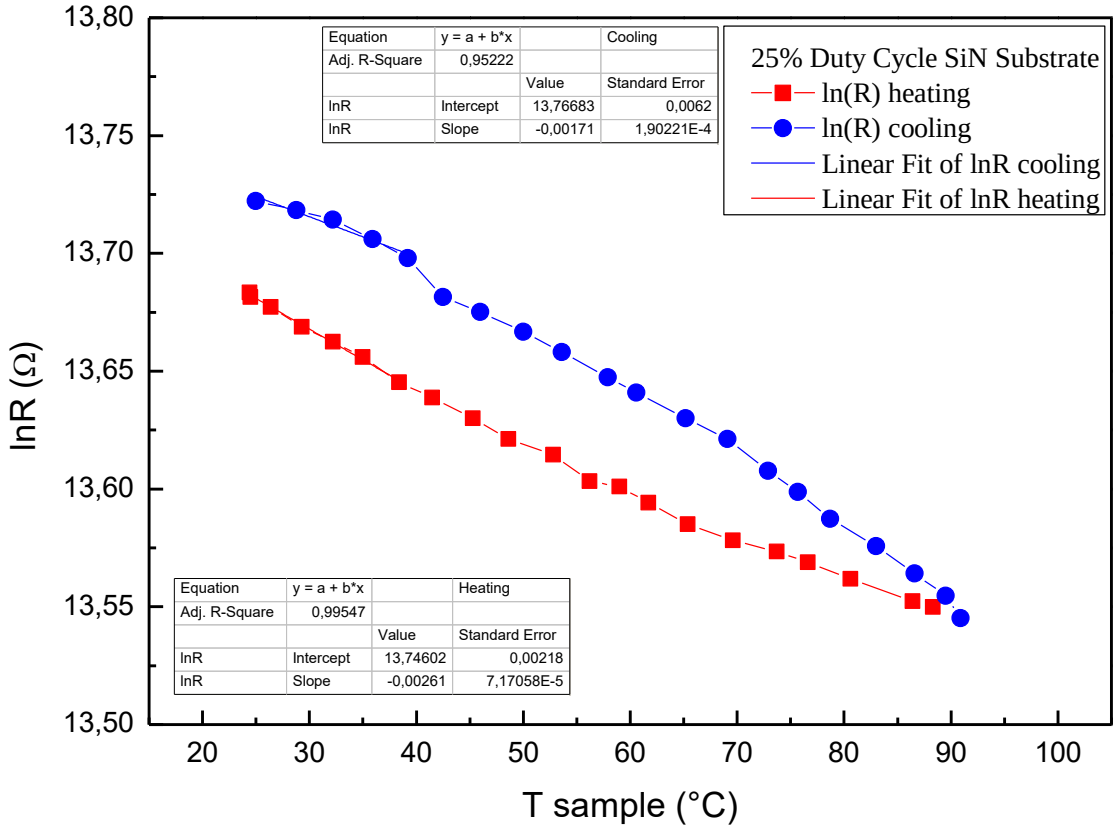

Figure 3.10. *(Continued) Change in lnR and R with respect to temperature for different samples deposited using duty cycle values*

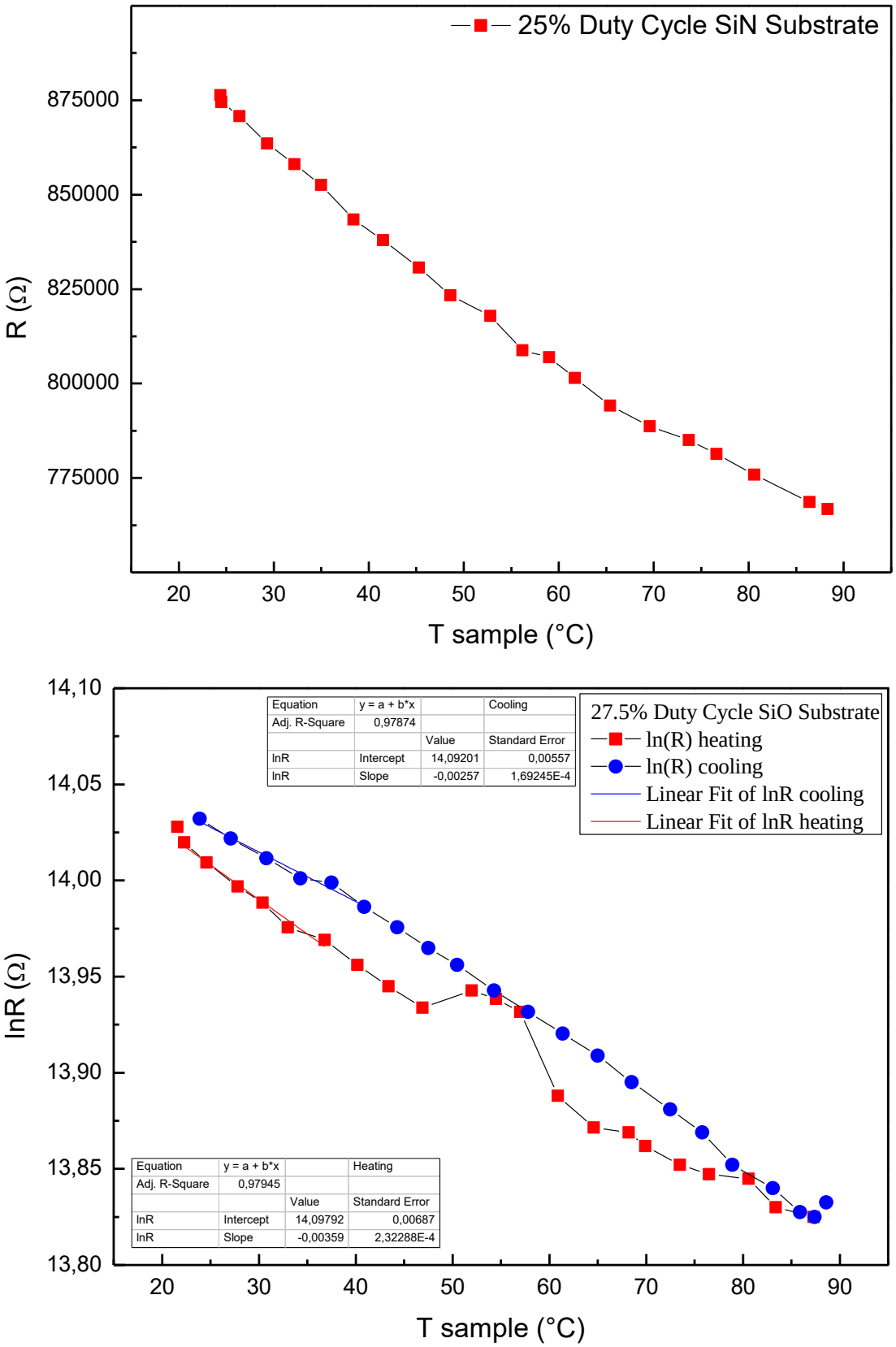

Figure 3.10. *(Continued) Change in lnR and R with respect to temperature for different samples deposited using duty cycle values*

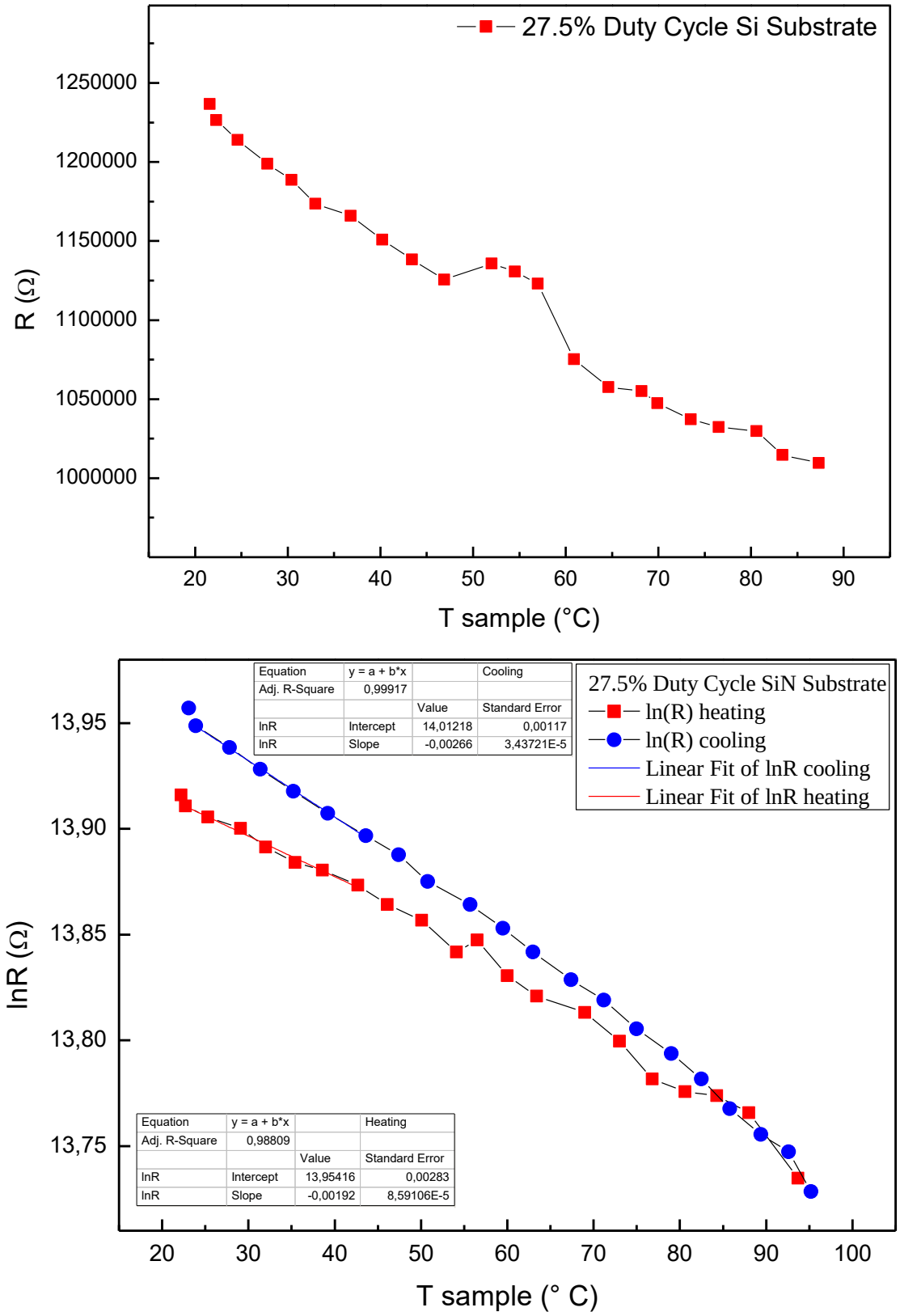

Figure 3.10. *(Continued) Change in lnR and R with respect to temperature for different samples deposited using duty cycle values*

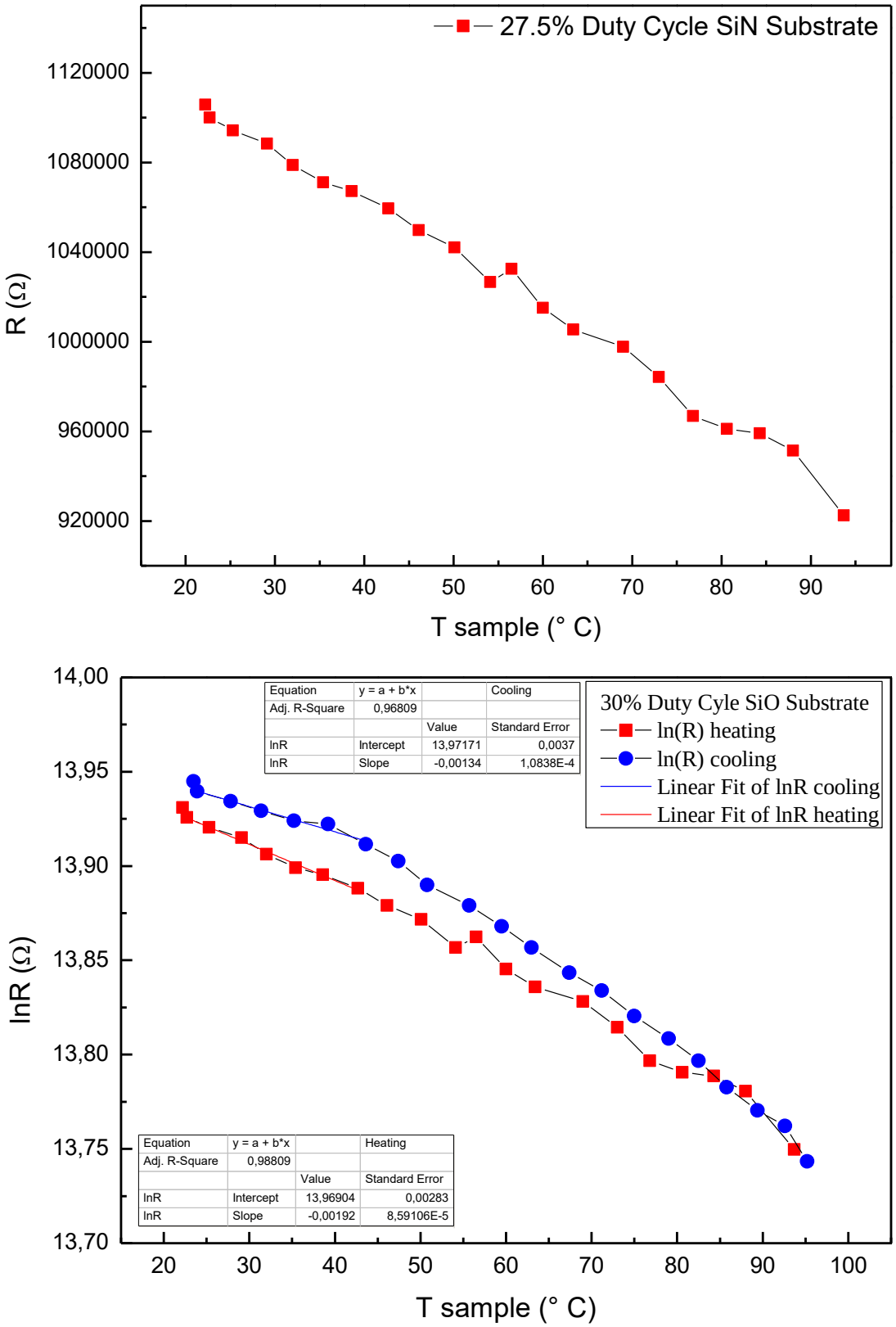

Figure 3.10. *(Continued) Change in lnR and R with respect to temperature for different samples deposited using duty cycle values*

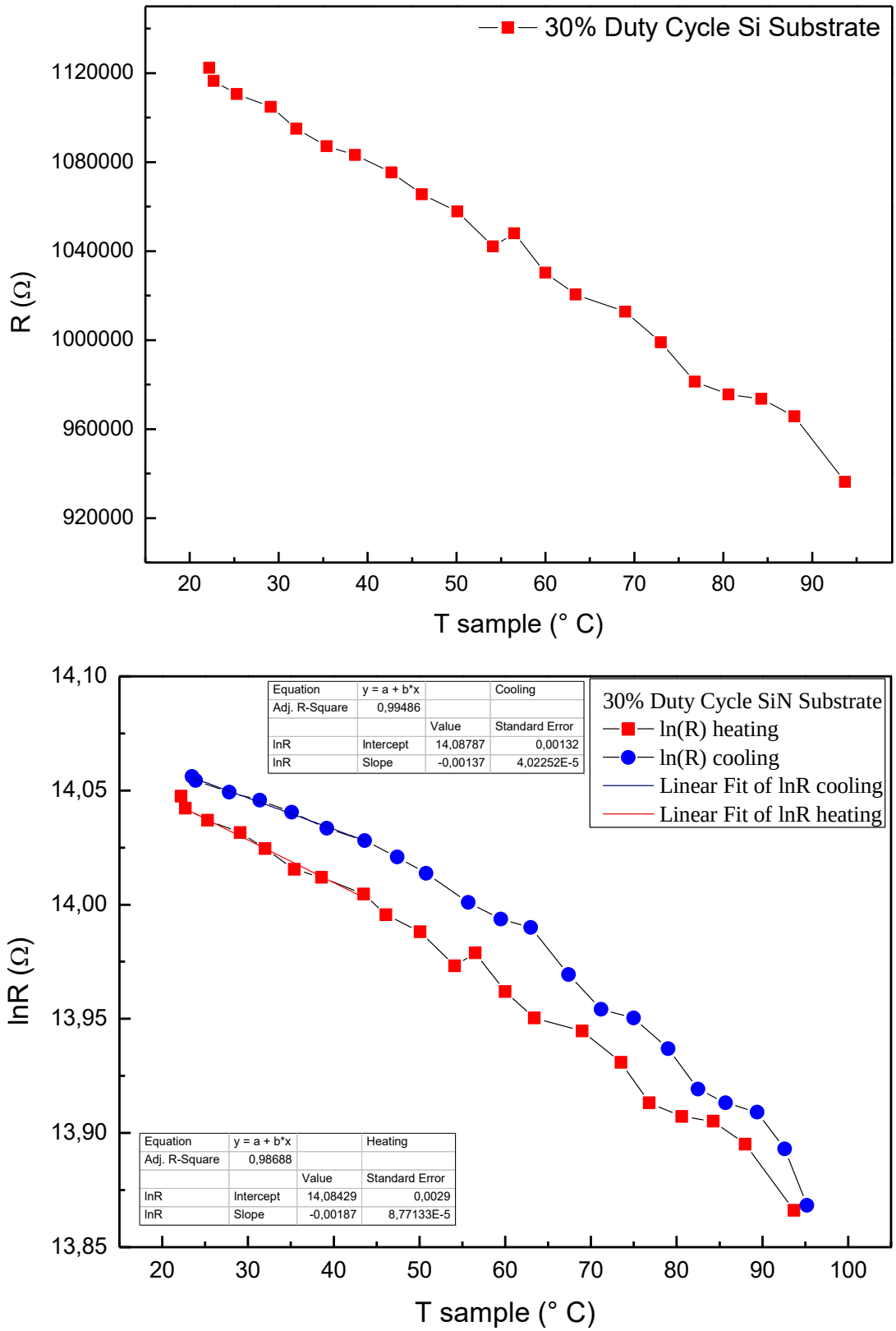

Figure 3.10. *(Continued) Change in lnR and R with respect to temperature for different samples deposited using duty cycle values*

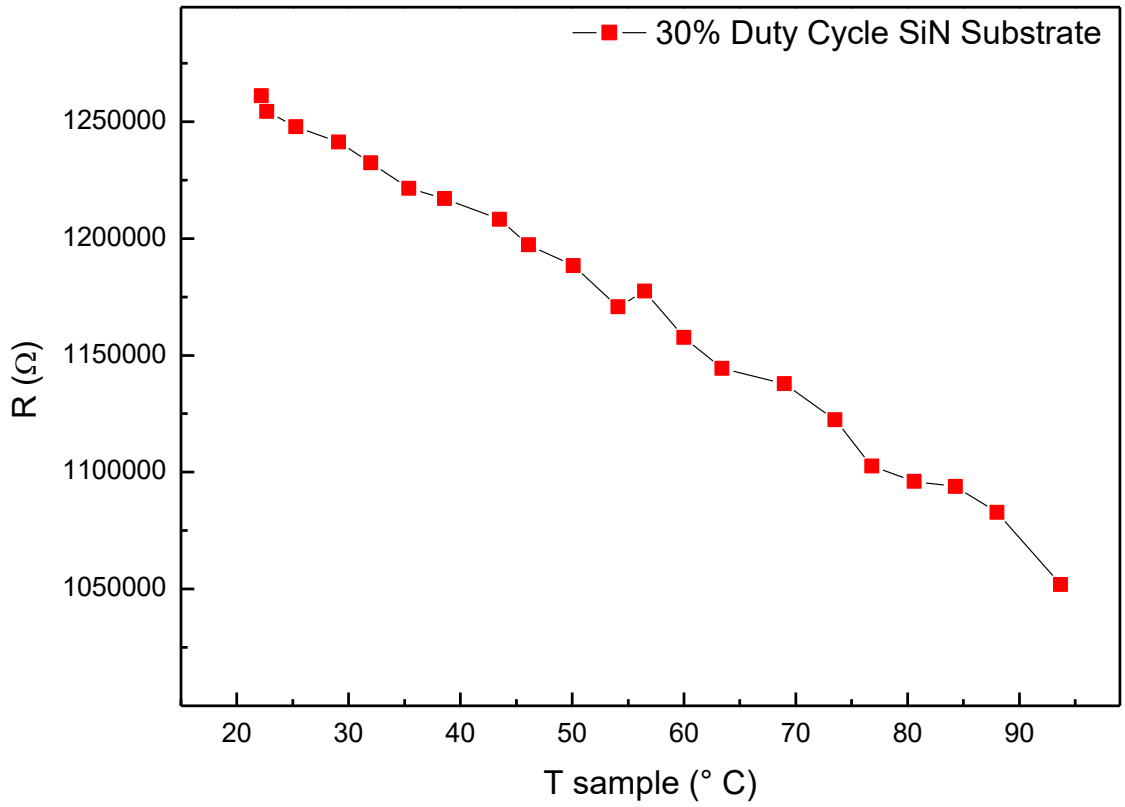

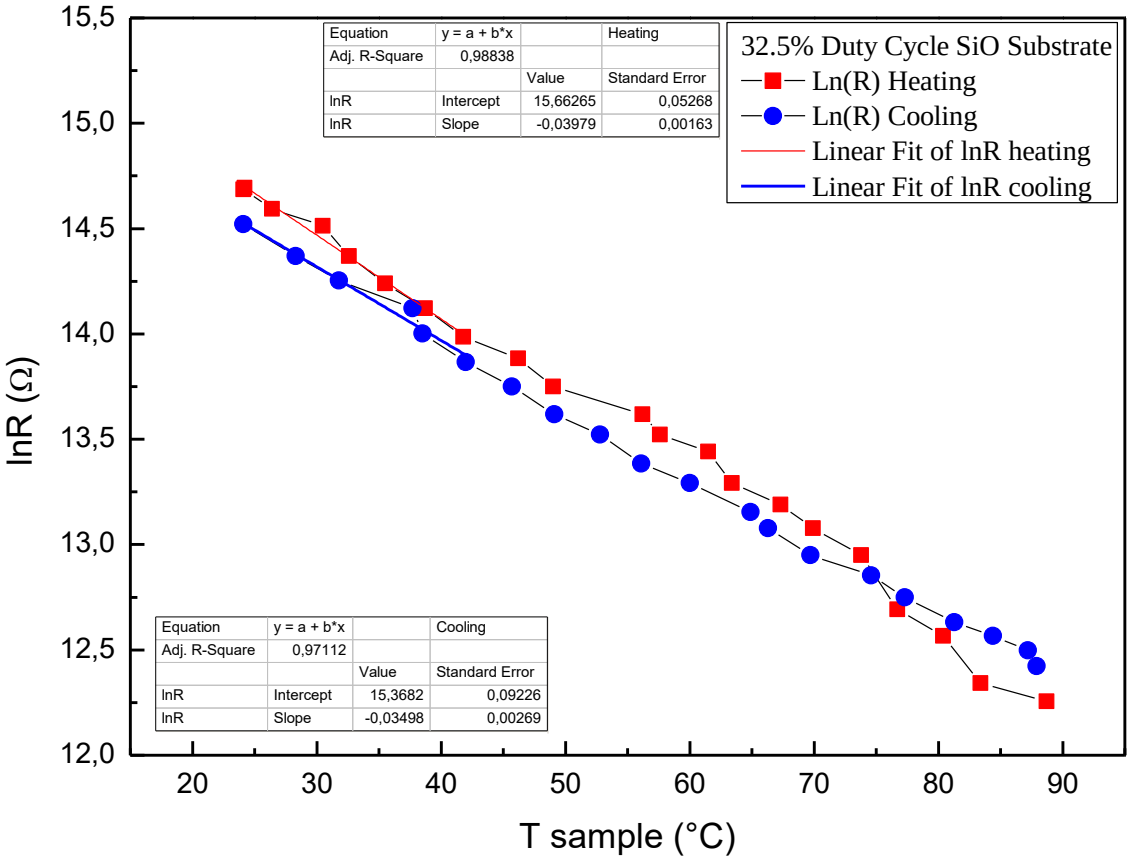

Figure 3.10. *(Continued) Change in lnR and R with respect to temperature for different samples deposited using duty cycle values*

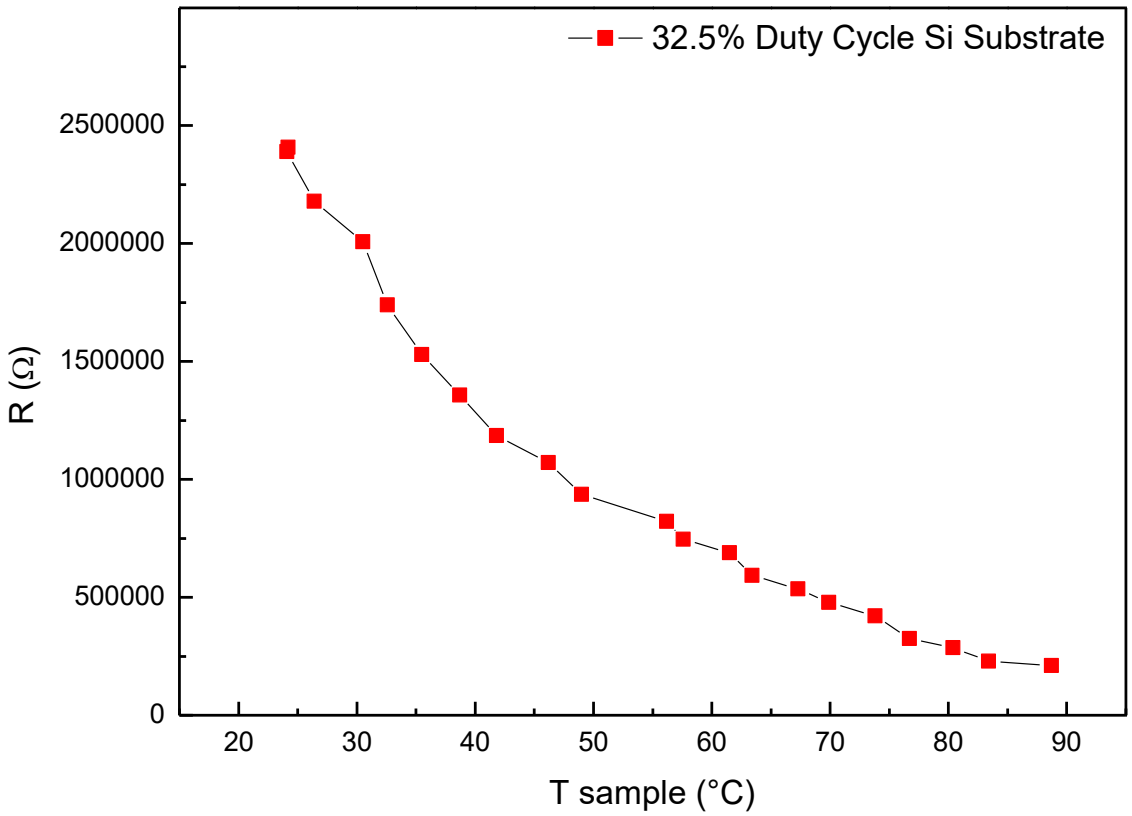

Figure 3.10. (Continued) Change in lnR and R with respect to temperature for different samples deposited using duty cycle values

Resistance change with respect to increasing temperature results show a near linear decreasing behavior, indicating a normal high resistance behavior except for the sample deposited with 25% duty cycle onto Si/SiO_2 substrate. This result suggests that O_2/Ar ratio is the effective parameter on semiconducting temperature resistance along with the findings of D. Ruzmetov and S. Ramanathan [14].

4. CONCLUSIONS

In this study effect of duty cycle on the properties of vanadium oxide thin films deposited with P-DC reactive magnetron sputtering is investigated. 16 samples are deposited on two different substrate types with 8 different duty cycle values. All other deposition parameters are kept constant. Samples are characterized with GI-XRD for phase and structure analysis, FPP for electrical characterization and AFM for surface properties and average grain size. TEM imaging is used on one sample to confirm crystallization.

Electrical characterization results indicate that resistance and resistivity of the vanadium oxide thin films are inversely proportional with duty cycle whereas no proportional relationship observed for TCR. The decline in resistance and resistivity with increasing duty cycle suggests that duty cycle is effective on both stoichiometry and structural defects. Decreasing trend in resistance and resistivity result is in agreement with the study of Xiang Dong et.al. but the correlation between TCR and duty cycle in their work have not been observed in this study. In the work of Xiang Dong et.al. glass slides as substrates and water cooled planar rectangle vanadium target with 99.99% purity is used and it is stated that the increase in reverse duty cycle enhances the oxidation of vanadium and it is more pronounced at higher oxygen flow [6]. 3.1% O_2/Ar ratio with high argon (100 sccm) and oxygen (3.1 sccm) flow rates had been used by Xiang Dong et.al. which is considerably low when compared with the 20% O_2/Ar ratio with 2 sccm argon and 0.4 sccm oxygen used in this study. Differences in flow rates and substrate types used may explain the disagreement in TCR findings between the two studies.

Regressive trend observed on surface roughness with increasing duty cycle supports the effect of duty cycle on morphology and may indicate an increase in structural uniformity as well.

GI-XRD results show an amorphous structure with one exception which is confirmed by TEM imaging. This indicates duty cycle is also effective on crystallization through altering the reaction kinetics by affecting excitation states of charged particles in plasma. More study is needed to prove the effect and to check for a correlation.

Another observation made during this study is the near linear decrease in resistance with respect to increasing temperature in samples with 20% to 30% duty cycles. This may be related to thermoresistive behavior. The hump observed between 50°C and 60°C, especially in the sample deposited on Si/SiO_2 substrate with 27.5% duty cycle may

indicate presence of VO_2 phase. The exponential decrease observed in samples with 10%, 15% and 32.5% duty cycles can be interpreted as semiconductive behavior. For better structure property correlation further detailed investigations by TEM and Raman Spectroscopy is needed.

REFERENCES

[1] Belkind, A., Zhao, Z., Carter, D., Mahoney, L., McDonough, G., Roche, G., Scholl, R. and Walde, H. (2000). Pulsed-DC reactive sputtering of dielectrics: pulsing parameter effects. In Proceedings of The Annual Technical Conference - Society Of Vacuum Coaters, pp. 86-90.

[2] Sellers, J. (1998). Asymmetric bipolar pulsed DC: the enabling technology for reactive PVD. Surface and Coatings Technology, 98(1-3), 1245-1250.

[3] Hsiao, Y. C., Lee, J. W., Yang, Y. C., & Lou, B. S. (2013). Effects of duty cycle and pulse frequency on the fabrication of AlCrN thin films deposited by high power impulse magnetron sputtering. Thin Solid Films, 549, 281-291.

[4] Bai, W. Q., Wang, X. L., Gu, C. D., & Tu, J. P. (2015). Influence of duty cycle on microstructure, tribological and corrosion behaviors of aC/aC: Ti multilayer films. Thin Solid Films, 584, 214-221.

[5] Rizzo, A., Valerini, D., Capodieci, L., Mirenghi, L., Di Benedetto, F., & Protopapa, M. L. (2018). Reactive bipolar pulsed dual magnetron sputtering of ZrN films: The effect of duty cycle. Applied Surface Science, 427, 994-1002.

[6] Dong, X., Wu, Z., Xu, X., Wang, T., & Jiang, Y. (2014). Effects of duty cycle and oxygen flow rate on the formation and properties of vanadium oxide films deposited by pulsed reactive sputtering. Vacuum, 104, 97-104.

[7] http-1: http://www.rsc.org/periodic-table/element/23/vanadium
(Date accessed: 10.12.2017)

[8] Lide, D. R. (2004). CRC Handbook of Chemistry and Physics 2004-2005: A Ready-Reference Book of Chemical and Physical Data.

[9] Yang, X., Cai, C., Zhou, S., Liu, H., & Liu, W. (2010). VOx films prepared by DC magnetron sputtering. Chinese Optics Letters, 8(s1), 137.

[10] Haber, J., Witko, M., & Tokarz, R. (1997). Vanadium pentoxide I. Structures and properties. Applied Catalysis A: General, 157(1-2), 3-22.

[11] Mui, S. C., Jasinski, J., Leppert, V. J., Mitome, M., Sadoway, D. R., & Mayes, A. M. (2006). Microstructure effects on the electrochemical kinetics of vanadium pentoxide thin-film cathodes. Journal of The Electrochemical Society, 153(7), A1372-A1377.

[12] Wang, X. J., Li, H. D., Fei, Y. J., Wang, X., Xiong, Y. Y., Nie, Y. X., & Feng, K. A. (2001). XRD and Raman study of vanadium oxide thin films deposited on

fused silica substrates by RF magnetron sputtering. Applied Surface Science, 177(1), 8-14.

[13] Chen, S., Ma, H., Yi, X., Wang, H., Tao, X., Chen, M., ... & Ke, C. (2004). Optical switch based on vanadium dioxide thin films. Infrared Physics & Technology, 45(4), 239-242.

[14] Ruzmetov, D., & Ramanathan, S. (2010). Thin film metal oxides: fundamentals and applications in electronics and energy.

[15] Ling, Z., Jianhui, T., Hao, F., & Jingzhong, C. (2011). Study on mixed vanadium oxide thin film deposited by RF magnetron sputtering and its application. Physics Procedia, 18, 73-76.

[16] Als-Nielsen, J., & McMorrow, D. (2011). Elements of modern X-ray physics. John Wiley & Sons.

[17] Inaba, K. (2008). X-ray thin-film measurement techniques. Overview. RigakuJ, 24(1).

[18] Smits, F. M. (1958). Measurement of sheet resistivities with the four-point probe. Bell Labs Technical Journal, 37(3), 711-718.

[19] Veeco Instruments Inc. (2004). MultiMode, S.P.M. Instruction Manual Nano Scope Software Version 5.

[20] Martin, P. M. (2009). Handbook of deposition technologies for films and coatings: science, applications and technology. William Andrew.

[21] Wasa, K., Kitabatake, M., & Adachi, H. (2004). Thin film materials technology: sputtering of control compound materials. Springer Science & Business Media.

[22] Muraoka, Y., & Hiroi, Z. (2002). Metal–insulator transition of VO 2 thin films grown on TiO 2 (001) and (110) substrates. Applied physics letters, 80(4), 583-585.

[23] Ruzmetov, D., Zawilski, K. T., Senanayake, S. D., Narayanamurti, V., & Ramanathan, S. (2008). Infrared reflectance and photoemission spectroscopy studies across the phase transition boundary in thin film vanadium dioxide. Journal of Physics: Condensed Matter, 20(46), 465204.

[24] Ruzmetov, D., & Ramanathan, S. (2010). Metal-insulator transition in thin film vanadium dioxide. In Thin Film Metal-Oxides (pp. 51-94). Springer US.

[25] Yağcı, A.M. (2015) Nano Ölçekli Vanadyum Oksit İnce Filmlerde Elektriksel Özelliklerinin Ve 1/f Gürültüsünün Karakterizasyonu, Yayımlanmamış Yüksek Lisans Tezi, Eskişehir: Anadolu Üniversitesi, Fen Bilimleri Enstitüsü.

[26] Advanced Energy Industries Inc. (2013). Pinnacle Plus+ 5 kW Power Supply 325 VDC-800VDC User Manual.

RESUME

PERSONAL DETAILS

Name, Surname	**:** Sinan Özgün
Birth Year and Place	: 1989, Eskişehir
Foreign Language	: English
E-mail	: sozgun@anadolu.edu.tr

EDUCATION

2015-2018	MSc at Anadolu University, Graduate School of Science, Materials Science and Engineering
2009-2014	BSc at Anadolu University, Faculty of Engineering, Materials Science and Engineering
2003-2008	Maltepe Military High School

WORK EXPERIENCE

2015-	Ford OTOSAN A.S., Inonu Plant, Powertrain Facility, Machining and Heat Treatment Manufacturing Engineer

VOLUNTEER EXPERIENCE

2009-	TED Conferences, Translator (English-Turkish)

PUBLICATIONS AND ACTIVITIES

2016, Poster Presentation, Effect of Load Distribution of Pinion Gear Spline Rolling Operation Racks on Differential Input Flange Runout, *Authors: S.Özgün, H.Özkara, M.Yalaman, M.Öge,* 7th International Symposium on Machining, Marmara University, December 3-5

2015, Poster Presentation, The Effects of Coating Thickness and O_2/Ar Flow Ratio on the Surface Morphology and Grain Size of Vanadium Oxide Thin Films Deposited by Pulsed DC Reactive Magnetron Sputtering, *Authors: S.Özgün, R.M.Öksüzoğlu, A.M.Yağcı, C.Yavru, E.Ayas*, NanoSmat Asia 2nd International Conference on Surfaces, Coatings and Nanostructured Materials, Kayseri, March 24-27

2015, Conference Presentation, Microstructure Evolution and Magnetic Properties of Nanocrystalline $Ni_{75}Fe_{25}$ Thin Films: Effect of Substrate and Thickness, *Authors: A. Kaibi, A. Guittoum, R.M. Öksüzoğlu, C. Yavru, S. Özgün, M. Boudissa, M. Kechouane,* NanoSmat Asia 2nd International Conference on Surfaces, Coatings and Nanostructured Materials, Kayseri, March 24-27

2015, Poster Presentation, Electrical Characterization of Nano-Size Grained Vanadium Oxide Thin Films, *Authors: E.Dirican, A.M.Yağcı, S.Özgün, C.Yavru, R.Kaçar, R.M.Öksüzoğlu*, 11th International Nanoscience and Nanotechnology Conference, METU, June 22-25

2014, Article, Modifying ultrafast optical response of sputtered VO_X nanostructures in broad spectral range by altering post annealing atmosphere, *Authors: U.Kürüm, H.G. Yaglioglu, B.Küçüköz, R.M.Öksüzoğlu, M.Yıldırım, A.M.Yağcı, C.Yavru, S.Özgün, T. Tıraş and A. Elmalı*, Journal of Optics, Volume 17, Number 1.